

Exploring the orthosymplectic zoo

Mohammad Akhond,^a Federico Carta,^b Siddharth Dwivedi,^c Hirotaka Hayashi,^d
Sung-Soo Kim^e and Futoshi Yagi^f

^a*Department of Physics, Swansea University,
Singleton Park, Swansea SA2 8PP, U.K.*

^b*Department of Mathematical Sciences, Durham University,
Durham DH1 3LE, U.K.*

^c*Center for Theoretical Physics, College of Physical Science and Technology, Sichuan University,
Chengdu 610064, China*

^d*Department of Physics, School of Science, Tokai University,
4-1-1 Kitakaname, Hiratsuka-shi, Kanagawa 259-1292, Japan*

^e*School of Physics, University of Electronic Science and Technology of China,
No. 2006, Xiyuan Ave, West Hi-Tech Zone, Chengdu, Sichuan 611731, China*

^f*School of Mathematics, Southwest Jiaotong University,
West Zone, High-tech District, Chengdu, Sichuan 611756, China*

E-mail: akhondmohammad@gmail.com, federico.carta@durham.ac.uk,
sdwivedi@scu.edu.cn, h.hayashi@tokai.ac.jp, sungsoo.kim@uestc.edu.cn,
futoshi_yagi@swjtu.edu.cn

ABSTRACT: We study the Higgs branch of the SCFT limit of 5d SO(6) and SO(8) gauge theory with hypermultiplets in the spinor and vector representations. In the case of SO(6) gauge theories, we contrast the magnetic quivers obtained with those of SU(4) gauge theory with hypermultiplets in the fundamental and second rank antisymmetric representations. Since SU(4) gauge theories admit several different values of the Chern-Simons level, we make some observations about how to distinguish those theories from the brane webs of the SO(6) theories. In the case of SO(8) gauge theories, we use SO(8) triality to propose (naively) inequivalent magnetic quivers, which will turn out to have the same moduli spaces of vacua, at least locally around their most singular loci. We encounter several interesting new phenomena occurring in the magnetic quivers, such as hypermultiplets between neighbouring symplectic gauge nodes and matter in two-index representations of unitary nodes. We also give a prescription for computing the local Coulomb branch Hilbert series for quivers involving bad USp(2) gauge nodes.

KEYWORDS: Brane Dynamics in Gauge Theories, Field Theories in Higher Dimensions, Field Theories in Lower Dimensions, Supersymmetric Gauge Theory

ARXIV EPRINT: [2203.01951](https://arxiv.org/abs/2203.01951)

Contents

1	Introduction	1
2	SO(6) vs. SU(4)	3
2.1	SO(6) theories without vector matter	5
2.1.1	$SO(6) + 2S/(1S + 1C) \longleftrightarrow SU(4)_{1/0} + 2F$	5
2.1.2	$SO(6) + 2S + 1C \longleftrightarrow SU(4)_{\frac{1}{2}} + 3F$	8
2.1.3	$SO(6) + 2S + 2C \longleftrightarrow SU(4)_0 + 4F$	9
2.1.4	$SO(6) + 3S + 2C \longleftrightarrow SU(4)_{\frac{1}{2}} + 5F$	11
2.1.5	$SO(6) + 3S + 3C \longleftrightarrow SU(4)_0 + 6F$	12
2.1.6	$SO(6) + 4S + 4C \longleftrightarrow SU(4)_0 + 8F$	13
2.2	SO(6) theories with a single vector hypermultiplet	14
2.2.1	$SO(6) + 2S/(1S + 1C) + 1V \longleftrightarrow SU(4)_{1/0} + 2F + 1AS$	14
2.2.2	$SO(6) + 2S + 1C + 1V \longleftrightarrow SU(4)_{\frac{1}{2}} + 3F + 1AS$	19
2.2.3	$SO(6) + 2S + 2C + 1V \longleftrightarrow SU(4)_0 + 4F + 1AS$	20
2.2.4	$SO(6) + 3S + 2C + 1V \longleftrightarrow SU(4)_{\frac{1}{2}} + 5F + 1AS$	22
2.2.5	$SO(6) + 3S + 3C + 1V \longleftrightarrow SU(4)_0 + 6F + 1AS$	23
2.2.6	$SO(6) + 4S + 4C + 1V \longleftrightarrow SU(4)_0 + 8F + 1AS$	23
2.3	SO(6) theories with two vector hypermultiplets	24
2.3.1	$SO(6) + 2S/(1S + 1C) + 2V \longleftrightarrow SU(4)_{1/0} + 2F + 2AS$	25
2.3.2	$SO(6) + 2S + 1C + 2V \longleftrightarrow SU(4)_{\frac{1}{2}} + 3F + 2AS$	27
2.3.3	$SO(6) + 2S + 2C + 2V \longleftrightarrow SU(4)_0 + 4F + 2AS$	28
2.3.4	$SO(6) + 3S + 2C + 2V \longleftrightarrow SU(4)_{\frac{1}{2}} + 5F + 2AS$	30
2.3.5	$SO(6) + 3S + 3C + 2V \longleftrightarrow SU(4)_0 + 6F + 2AS$	31
3	SO(8) triality	32
3.1	$SO(8) + 1V \longleftrightarrow SO(8) + 1S$	32
3.2	$SO(8) + 2V \longleftrightarrow SO(8) + 2S$	33
3.3	$SO(8) + 2S + 1C \longleftrightarrow SO(8) + 2S + 1V \longleftrightarrow SO(8) + 1S + 2V$	35
3.4	$SO(8) + 2S + 2C \longleftrightarrow SO(8) + 2S + 2V$	36
3.5	$SO(8) + 1S + 1C + 2V \longleftrightarrow SO(8) + 2S + 1C + 1V$	37
3.6	$SO(8) + 2S + 2C + 1V \longleftrightarrow SO(8) + 2S + 1C + 2V$	38
4	Conclusion	39
A	Unrefined Hilbert series results for OSp quivers	40

1 Introduction

Superconformal field theories (SCFTs) in five spacetime dimensions have received much deserved attention in recent years. Their mere existence forces us to expand our view of quantum field theories, as these fixed points cannot be reached by traditional means of perturbing around free field Lagrangians. Yet, by now, there is overwhelming evidence to support their existence, mostly due to stringy constructions starting with the seminal papers [1–4]. Broadly speaking, there are three independent, yet complementary points of view for studying these SCFTs, namely their embedding into type IIB brane webs [5–25], geometric engineering [2, 26–34] and holography [35–41].

Many 5d SCFTs, admit supersymmetry preserving mass deformations, which trigger an RG flow, whose low energy dynamics is effectively captured by an $\mathcal{N} = 1$ gauge theory. Such deformations, preserve the $SU(2)_R$ symmetry, while breaking the flavour symmetry. An important dynamical question is therefore to determine the full global symmetry of the parent SCFT of a given 5d gauge theory. 5d SCFTs and gauge theories, can possess a Higgs branch of their moduli space of vacua, which in the gauge theory regime can be constructed as the hyperKähler quotient [42, 43]. In the SCFT limit, the hyperKähler quotient, is no longer accessible, due to a lack of a Lagrangian description, making the study of the Higgs branch in this limit more challenging. There are, by now, a plethora of techniques to determine the enhanced global symmetry of the SCFT parent of a given 5d gauge theory, such as 7-brane analysis [44–49], superconformal indices [50–52], as well as geometric approaches [2, 26–28, 53–58]. One particularly elegant approach to determine the SCFT flavour symmetries as well as the Higgs branch of the SCFT, pioneered in [59], is to consider their magnetic quivers. The magnetic quiver (MQ), of a given 5d theory, is a 3d $\mathcal{N} = 4$ quiver gauge theory, whose Coulomb branch is isomorphic to the Higgs branch of the 5d theory in question. In many cases, though not always, one can show that the magnetic quiver of a given 5d theory, is the 3d mirror of its torus compactification. This leads to an interesting interplay between 5d $\mathcal{N} = 1$ theories and 3d $\mathcal{N} = 4$ theories, and has prompted many recent studies [59–78].

That 3d magnetic quivers are advantageous, is due to recent advances in extracting the algebraic geometry of 3d $\mathcal{N} = 4$ Coulomb branches [79–83]. Coulomb branches of 3d $\mathcal{N} = 4$ theories, are parameterised by BPS monopole operators, whose R-charges can be determined from the R-charges of the fermionic content of the theory [84]. Following the terminology of Gaiotto and Witten [85], we refer to a 3d $\mathcal{N} = 4$ theory as good, ugly or bad, depending on the conformal dimension of the monopole operators in that theory. A theory is said to be good, if the conformal dimension of all monopole operators is greater than $\frac{1}{2}$, which is the dimension of a scalar in (2+1) dimensions. A bad theory is one in which some monopole operator has a conformal dimension less than $\frac{1}{2}$. Finally, in an ugly theory, there are some monopole operators whose conformal dimension is exactly $\frac{1}{2}$, but none that are smaller. For good or ugly theories, the monopole formula [79], can correctly produce the Hilbert series of the Coulomb branch, using the UV gauge theory data. However, for bad theories, the monopole formula fails, due to the fact that the UV R-symmetries of the theory are different from the superconformal R-symmetry, and hence the UV R-

charge cannot be used to predict the conformal dimension of the SCFT operators. The full structure of the Coulomb branch of some bad theories was recently understood by Assel and Cremonesi in [86, 87], building on earlier results in [88, 89]. In particular, it was found that for $\mathrm{USp}(2N)$ SQCD with $2N$ flavours in the fundamental representation, the Coulomb branch has two most singular points, where the theory flows to an interacting SCFT in the deep infra-red, with a local mirror Lagrangian in the vicinity of each singular point. This is unlike the situation for good theories, where the most singular point on the moduli space is unique, namely the origin, with an SCFT at the bottom of the RG flow in that vacuum. The Coulomb branch Hilbert series of the local geometry around one of the two most singular points of the $\mathrm{USp}(2N)$ SQCD with $2N$ flavours was computed in [87], and shown to agree with the Higgs branch Hilbert series of the local mirror.

The goal of this paper is to illuminate the Higgs branch of the SCFT parents of 5d gauge theories whose gauge group is either $\mathrm{SO}(6)$, or $\mathrm{SO}(8)$, and with matter in the vector, spinor, and conjugate spinor representations. Our motivation is partly due to the fact that, among classical simple gauge groups, the magnetic quivers for A_N and C_N cases are well studied [59, 90], while those of B_N and D_N remain relatively unexplored. The magnetic quivers for $\mathrm{SO}(N)$ gauge theories with matter in vector representation were recently constructed in [62], using their embedding into brane webs with $\mathrm{O}7^+$ -planes. The current work complements this study by adding matter in the spinor and the conjugate spinor representations. The reason for restricting the rank of the gauge group is mostly for practical reasons. The construction of magnetic quivers from brane webs with $\mathrm{O}5$ -planes is, at present, still not completely systematic. It is, therefore, useful to limit the discussion to situations where a consistency check of our computations is available. For $\mathrm{SO}(6)$ gauge theories, this is achieved by comparing the orthosymplectic magnetic quivers obtained from brane webs with an $\mathrm{O}5$ -plane, with the unitary magnetic quivers obtained from the brane webs of $\mathrm{SU}(4)$ gauge theories. Similarly, for $\mathrm{SO}(8)$ gauge theories, one can set up a consistency check, by exploiting $\mathrm{SO}(8)$ triality. As we shall see, in the rest of this paper, such considerations also lead to some interesting results for 3d $\mathcal{N} = 4$ theories. In particular, in section 2, we exploit the isomorphism between $\mathrm{SO}(6)$ and $\mathrm{SU}(4)$, to conjecture exact highest weight generating functions for orthosymplectic magnetic quivers, simply by carrying over the results from their unitary counterparts. Similarly, in section 3, we uncover several intriguing equalities of moduli spaces, of naively unrelated quivers.

Throughout the paper, we encounter magnetic quivers which contain bad $\mathrm{USp}(2N)$ nodes, where the effective number of hypermultiplets is exactly $2N$. We devise a method to associate a Hilbert series to these quivers, by using the local mirror description around one of their two most singular loci. We will refer to this procedure of associating the Coulomb branch Hilbert series of a good theory, to the local geometry of the Coulomb branch near a singular locus of a bad theory as “B2G”. For the specific case of $\mathrm{USp}(2)$ with 2 flavours, the prescription is first encountered in section 2.2.1. A similar prescription for $\mathrm{USp}(2N)$ theories for $N \geq 2$ is used throughout the paper, though the technical details will be published elsewhere [91]. The validity of our prescription is confirmed, by comparing the results with those computed using the Hall-Littlewood technique [80]. In addition, many of the magnetic quivers that involve bad nodes, can have a good “dual” description,

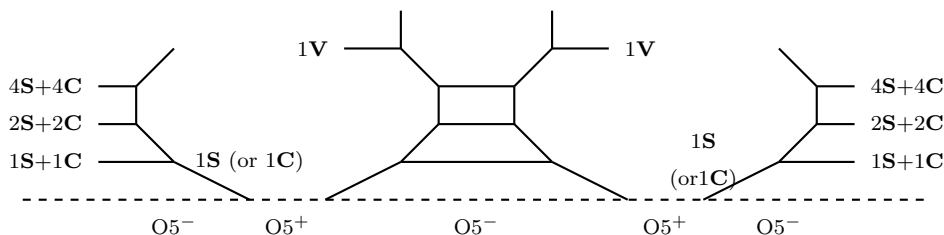


Figure 1. A web diagram for $SO(6)+2V$ with various spinor matters.

since we have several inequivalent brane constructions for each 5d theory we consider. The Hilbert series computed using our proposed prescription, is also consistent with the good “dual” quivers.

The content of the remainder of this paper is organised as follows: section 2 contains MQs for $SO(6)$ gauge theories derived from brane webs with $O5$ -planes, as well as MQs for $SU(4)$ theories, derived from ordinary brane webs. Here we will encounter MQs with bad symplectic gauge nodes and devise various methods to extract the good interacting part. Section 3 is dedicated to studying the MQs for $SO(8)$ theories, and a comparison is made between MQs of $SO(8)$ theories related by triality, exchanging spinor, conjugate spinor, and vector representations of $SO(8)$. We conclude with our wish list for future projects in section 4. Appendix A contains the unrefined Hilbert series results for the orthosymplectic ($O\text{Sp}$) quivers.

2 $SO(6)$ vs. $SU(4)$

In this section, we consider magnetic quivers for 5d SCFTs that admit a mass deformation, such that their low-energy dynamics is captured by $SO(6)$ gauge theory with s hypermultiplets in the spinor representation \mathbf{S} , c hypermultiplets in the conjugate spinor representation \mathbf{C} and v hypermultiplets in the vector representation \mathbf{V} of $SO(6)$. Since the Lie algebra of $SO(6)$, is isomorphic to the Lie algebra of $SU(4)$, the low-energy theory may also be thought of as $SU(4)$ gauge theory, with $(s+c)$ hypermultiplets in the fundamental representation \mathbf{F} , and v hypermultiplets in the 2nd rank antisymmetric representation \mathbf{AS} of $SU(4)$. The Chern-Simons level for the $SU(4)_\kappa$ gauge theory is given by $\kappa = \frac{s-c}{2}$:

$$SO(6) + s\mathbf{S} + c\mathbf{C} + v\mathbf{V} \leftrightarrow SU(4)_{\frac{s-c}{2}} + (s+c)\mathbf{F} + v\mathbf{AS}. \quad (2.1)$$

One can engineer $SO(6)+s\mathbf{S}+c\mathbf{C}+v\mathbf{V}$ using a five-brane web with an $O5$ -plane. In particular, (conjugate) spinors are introduced as a separate web on the left or right side of an $SO(6)$ five-brane web as given in figure 1. This web can be viewed as a quiver theory $USp(0)-SO(6)-USp(0)$, where the $USp(0)$ instanton, plays the role of the spinor matter [12]. Notice that in figure 1, only restricted configurations of spinors and conjugate spinors are possible. For instance, $4\mathbf{S}+3\mathbf{C}$ cannot be depicted as a five-brane web. Furthermore, the distinction between spinors and conjugate spinors needs some caution. For instance, consider a five-web with two spinors, as shown in figure 2. This web can have three different

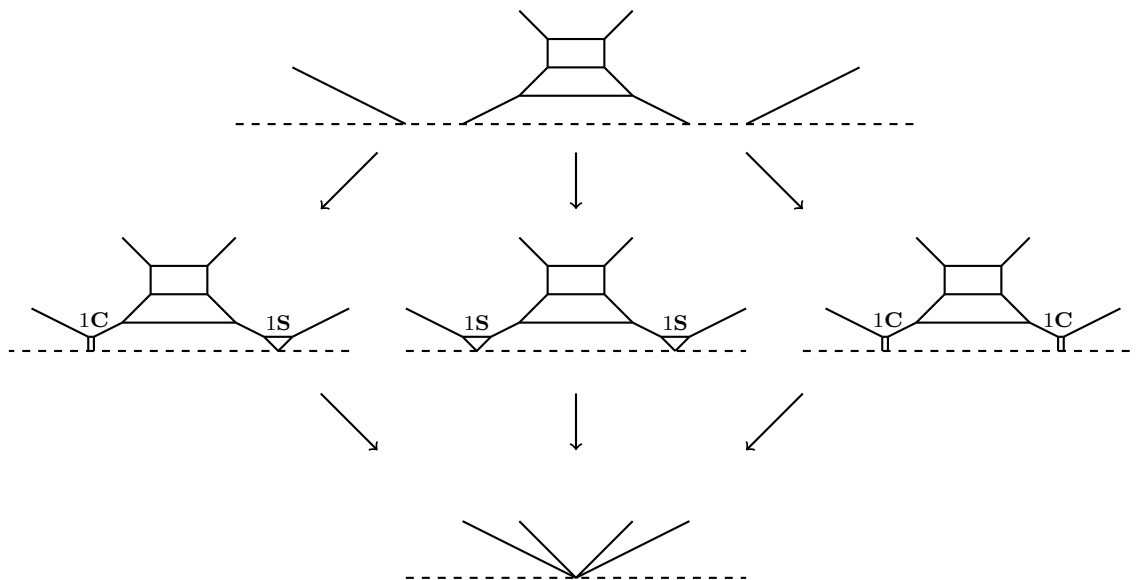


Figure 2. 5-brane webs for the $SO(6)$ with three possible spinor configurations. The web diagram on the top is generic 5-brane web depicted with an $O5$ -plane (dotted line) where spinors are introduced on the left and right. The 5-brane webs in the middle are three possible brane configurations, $1S+1C$, $2S$, and $2C$. The web on the bottom is the 5-brane configuration at infinite coupling.

interpretations, depending on how the configuration undergoes the “generalized flop” transition [20] when two spinor webs are brought towards the centre of the Coulomb branch. In particular, $1S$ is modified into the web for the E_1 theory, while $1C$ is modified into the web for the \tilde{E}_1 theory [20, 60]. In figure 2, we depict three possible configurations, $1S+1C$, $2S$, and $2C$. We stress that the corresponding webs in the infinite coupling limit all look the same, and hence one needs to distinguish them by hand.

One can engineer $SU(4)_{\frac{s-c}{2}} + (s+c)\mathbf{F} + v\mathbf{AS}$, using a five-brane web description without an $O5$ -plane [10]. Taking the SCFT limit of the two brane webs, of the $SO(6)$ and $SU(4)$ theories, and reading off the corresponding magnetic quivers following the techniques developed in [60, 61, 90] yields two dual descriptions for the Higgs branch of the 5d SCFT in question. The magnetic quivers obtained from the brane web with an $O5$ -plane will have qualitatively different features, compared to the magnetic quivers obtained from the brane webs without an $O5$ -plane. Typical features of magnetic quivers obtained from brane webs with an $O5$ -plane are the presence of orthogonal, and symplectic gauge nodes, hypermultiplets in the fundamental-fundamental representation of two unitary nodes, and hypermultiplets in the second rank symmetric or antisymmetric representation of unitary nodes. In contrast, the magnetic quivers obtained from ordinary brane webs will only contain unitary nodes and bi-fundamental matter, with the possibility of multiple links (bi-fundamental hypermultiplets) connecting two gauge nodes.

In what follows, we will often encounter theories, whose Higgs branch is given as the union of several cones, where each cone is described by a distinct magnetic quiver. We will denote by $MQ_i^{s,c,v}$, the magnetic quiver for the i -th cone of the SCFT parent of $SO(6)$

$+s\mathbf{S}+c\mathbf{C}+v\mathbf{V}$, i.e.,

$$\mathcal{H}_{\infty}^{5d}(\text{SO}(6) + s\mathbf{S} + c\mathbf{C} + v\mathbf{V}) = \bigcup_i \mathcal{C}^{3d}(\text{MQ}_i^{s,c,v}). \tag{2.2}$$

Our notation for the magnetic quivers follows those of [60, 62], which we now briefly review for the reader’s convenience. We use a circular white, red, or blue node to denote a unitary, orthogonal, or symplectic gauge algebra (and hence a 3d $\mathcal{N} = 4$ vector multiplet) respectively. Square nodes with the same colour-coding are used to denote flavour symmetries. We label each node by the dimension of the fundamental representation of the corresponding algebra. A solid line connecting two nodes, represents a hypermultiplet transforming in the bi-fundamental representation of the nodes that it connects. An exception to the previous statement is the case in which a solid line connects a symplectic and orthogonal node, in that instance one has to impose a reality condition which leads to a half hypermultiplet in the fundamental-fundamental representation. We use a dashed line connecting two unitary gauge nodes to represent hypermultiplets transforming under the fundamental-fundamental representation. A link starting and ending on a unitary gauge node represents hypermultiplets in the second rank antisymmetric representation, the number of such hypermultiplets will be written explicitly in the diagrams. Hypermultiplets in the second rank symmetric representation of unitary gauge nodes are denoted by jagged lines.

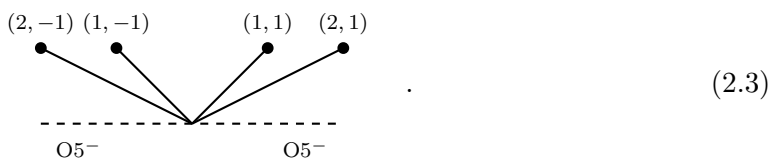
The rest of this section is further subdivided to the cases with $v = 0, 1, 2$.

2.1 SO(6) theories without vector matter

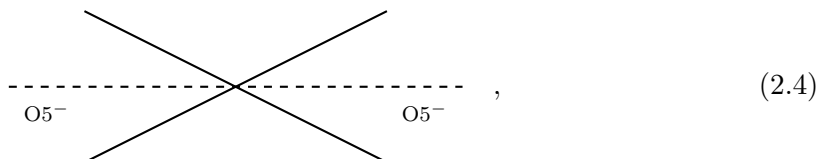
We will first consider SO(6) theories, with (conjugate) spinors and without any vector hypermultiplets. The unitary magnetic quivers correspond to $\text{SU}(4)_{\kappa}$ with fundamental hypermultiplets, and were given explicitly in [74]. All the magnetic quivers appearing in this section have a simple highest weight generating function (HWG) [83] for their Coulomb branch Hilbert series. We verify that the same HWG can correctly reproduce the unrefined Hilbert series of the Coulomb branch of the OSp quivers.

2.1.1 SO(6) + 2S/(1S + 1C) \longleftrightarrow SU(4)_{1/0} + 2F

The brane web for SO(6)+2S at infinite coupling is given by



This diagram can actually represent two distinct theories, namely, SO(6)+2S, as well as SO(6)+1S+1C. The easiest way to see this, is to realise that (2.3) contains the following subweb



which can either be the strong coupling limit of $\text{USp}(2)_0$, or that of $\text{USp}(2)_\pi$, depending on how one performs a generalized flop in going to the gauge theory phase [20, 60]. Therefore, this decomposition gives rise to two magnetic quivers, depending on whether one treats the subweb comprised of the $(2, 1)$ and $(2, -1)$ 5-branes as the strongly coupled limit of $\text{USp}(2)_0$ or $\text{USp}(2)_\pi$ gauge theory. In the former case, the subweb in question is dynamical, and gives rise to a gauge node of rank one in the magnetic quiver, while in the latter we treat this subweb as frozen, and it only contributes as a flavour node in the magnetic quiver, whose rank is determined by taking its intersection number with the remaining subweb made up of the $(1, 1)$ and $(1, -1)$ 5-branes. In addition, we can consider the subweb decomposition

(2.5)

giving rise to a total of three magnetic quivers that one can extract from the diagram (2.3). A comparison with the unitary magnetic quivers, obtained from the brane webs for $\text{SU}(4)_0+2\mathbf{F}$, and $\text{SU}(4)_1+2\mathbf{F}$, allows us to recognise the magnetic quiver for $\text{SO}(6)+1\mathbf{S}+1\mathbf{C}$ to be

$$\text{MQ}_1^{1,1,0} = \begin{array}{c} \square^1 \\ | \\ \circ^1 \text{---} \circ^1 \\ | \\ \square^1 \end{array}, \quad (2.6)$$

while the magnetic quivers for $\text{SO}(6)+2\mathbf{S}$ are given by

$$\text{MQ}_1^{2,0,0} = \begin{array}{c} \circ^1 \text{---} \circ^1 \\ | \\ \square^2 \end{array}, \quad \text{MQ}_2^{2,0,0} = \begin{array}{c} \square^2 \\ | \\ \circ^1 \end{array}. \quad (2.7)$$

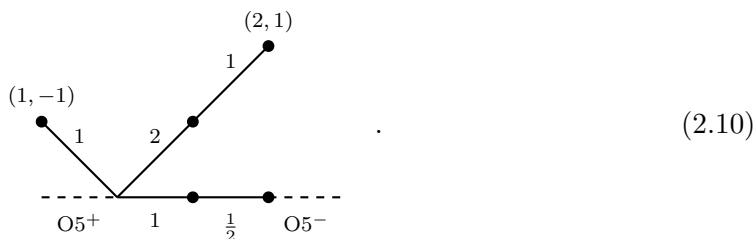
To confirm this, let us consider the brane web for $\text{SU}(4)_0+2\mathbf{F}$ at infinite coupling

(2.8)

The magnetic quiver one reads from this brane web is

$$\begin{array}{c} \circ^1 \\ / \quad \backslash \\ \circ^1 \text{---} \circ^1 \end{array}, \quad (2.9)$$

which we claim to be the same theory, in a sense to be clarified shortly, as $\text{MQ}_1^{1,1,0}$. In addition, we can consider, yet another web diagram, for the infinite gauge coupling limit of $\text{SO}(6)+1\mathbf{S}+1\mathbf{C}$

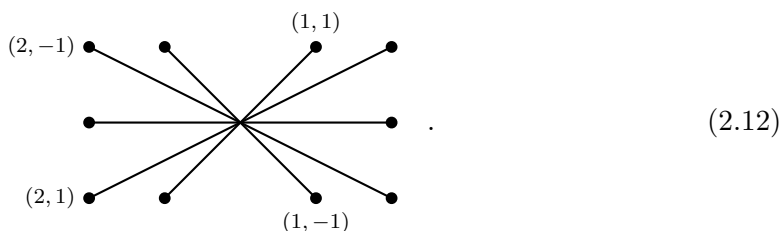


The magnetic quiver that one obtains from this brane system is



which is trivially the same as (2.9), upon removing the overall decoupled $\text{U}(1)$.

Consider now, the brane web for the SCFT limit of $\text{SU}(4)_1+2\mathbf{F}$



From here, one can read off the following pair of magnetic quivers



which can easily be identified with $\text{MQ}_1^{2,0,0} \cup \text{MQ}_2^{2,0,0}$ (2.7), modulo field redefinitions. The Coulomb branch and Higgs branch Hilbert series of $\text{MQ}_1^{1,1,0}$, $\text{MQ}_1^{2,0,0}$ and $\text{MQ}_2^{2,0,0}$ match with their unitary counterparts and the unrefined results are given in table 3 and table 4 respectively. The HWG for these magnetic quivers takes a very simple form and is given by

$$\begin{aligned} \text{HWG}_C(\text{MQ}_1^{1,1,0}) &= \text{HWG}_C(2.9) = \text{PE} \left[(1 + \mu^2)t^2 + (q + q^{-1})\mu t^4 - \mu^2 t^8 \right], \\ \text{HWG}_C(\text{MQ}_1^{2,0,0}) &= \text{HWG}_C^1(2.13) = \text{PE} \left[t^2 + (q + q^{-1})t^4 - t^8 \right], \\ \text{HWG}_C(\text{MQ}_2^{2,0,0}) &= \text{HWG}_C^2(2.13) = \text{PE} \left[\mu^2 t^2 \right], \end{aligned} \tag{2.14}$$

where in the above, we use μ to denote the highest weight fugacity for $\text{SU}(2)$, and q as a $\text{U}(1)$ fugacity.

We will now present an intuitive argument, for the agreement of the Hilbert series of the two apparently different quivers in (2.6) and (2.9). These quivers actually describe the same 3d $\mathcal{N} = 4$ theory. The only reason for which they look different, is that the

	U(1) ₁	U(1) ₂
Q ₁	1	-1
Q ₂	1	1
Q ₃	2	0

Table 1. Table of charges for the hypermultiplets in theory (2.6).

	$\tilde{U}(1)_1$	$\tilde{U}(1)_2$	$a\tilde{U}(1)_1 + b\tilde{U}(1)_2$	$c\tilde{U}(1)_1 + d\tilde{U}(1)_2$
\tilde{Q}_1	1	0	a	c
\tilde{Q}_2	1	-1	$a - b$	$c - d$
\tilde{Q}_3	0	1	b	d

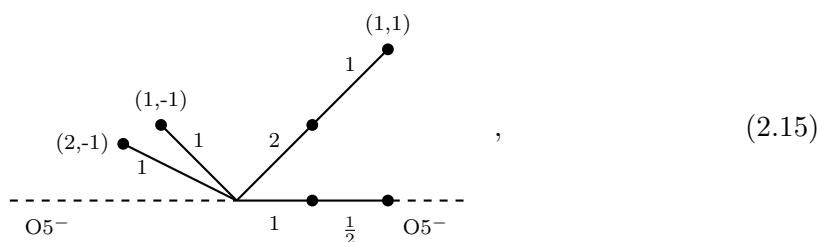
Table 2. Table of charges for the hypermultiplets in theory (2.9). In the last two columns we define two different U(1)s, whose Lie algebra generators are a linear combination of the generators of $\tilde{U}(1)_1$ and $\tilde{U}(1)_2$.

two abelian quivers are written considering U(1) charges of the hypermultiplets under two different sets of U(1)s. Said in other words, a simple change of basis in the Lie algebra of $U(1)^2$ can recast the table of charges of (2.9) into that of (2.6). We collect the charges of the various hypermultiplets in tables 1 and 2.

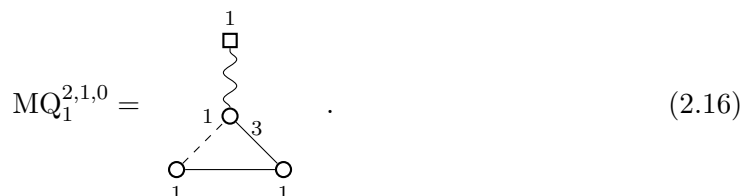
We notice that we can reproduce the U(1) charges of table 1 by taking $a = 1, b = c = d = -1$ in table 2. We will then identify Q_1 with \tilde{Q}_1, Q_3 with $\tilde{Q}_2,$ and finally Q_2 with the charge conjugate of \tilde{Q}_3 . In particular we remark that it is consistent to identify Q_2 and the charge conjugate of \tilde{Q}_3 , as each hypermultiplet consists of two chiral multiplets in conjugated gauge representations.

2.1.2 $SO(6) + 2S + 1C \longleftrightarrow SU(4)_{\frac{1}{2}} + 3F$

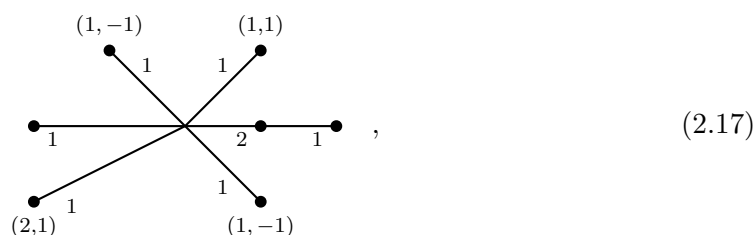
The brane web for $SO(6)+2S+1C$ at infinite gauge coupling limit is given by



from which we read off the following magnetic quiver



Next, we consider the web diagram for $SU(4)_0+3\mathbf{F}$



whose magnetic quiver is readily obtained to be



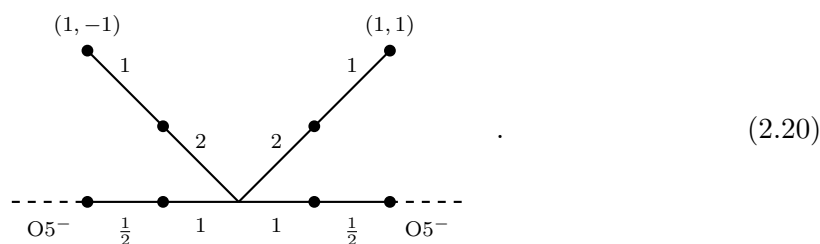
The unrefined computations of the Coulomb branch and Higgs branch Hilbert series for the two quivers match and are given in table 3 and table 4 respectively. The Coulomb branch and the Higgs branch of the above two quivers are identical with the following HWG:

$$HWG_C = HWG_H = PE \left[(1 + \mu_1\mu_2)t^2 + (\mu_1q + \mu_2q^{-1})t^4 - \mu_1\mu_2t^8 \right], \quad (2.19)$$

where μ_i are the highest weight fugacities of $SU(3)$ and q is the $U(1)$ charge. We remark that the duality between (2.18) and (2.16) generalises to the case in which the three bifundamental hypermultiplets among the $U(1)$ nodes are replaced with an arbitrary number n of them.

2.1.3 $SO(6) + 2\mathbf{S} + 2\mathbf{C} \longleftrightarrow SU(4)_0 + 4\mathbf{F}$

There are two inequivalent brane webs with $O5^-$ -plane that realise $SO(6)+2\mathbf{S}+2\mathbf{C}$. The first web diagram, involves a configuration with the orientifold plane asymptotically an $O5^-$ on both ends, corresponding to the 5d electric quiver $[1\mathbf{S} + 1\mathbf{C}] - SO(6) - [1\mathbf{S} + 1\mathbf{C}]$



The corresponding magnetic quiver is

$$MQ_1^{2,2,0} \cup MQ_2^{2,2,0} = \left(\text{quiver with nodes } 1, 2, 1, 2 \text{ and edges } 2, 2, 2 \right) \cup \left(\text{quiver with nodes } 4, 2 \text{ and edge } 2 \right), \quad (2.21)$$

where \wedge^2 denotes the rank 2 antisymmetric tensor. Alternatively, one can consider a brane web with an O5-plane which is asymptotically an O5⁺-plane on one end, and an O5⁻-plane on the other end

$$(2.22)$$

corresponding to the 5d IR quiver $SO(6) - [2S + 2C]$. From this web diagram we find an alternative magnetic quiver

$$\widehat{MQ}_1^{2,2,0} \cup \widehat{MQ}_2^{2,2,0} = \dots \cup \dots \quad (2.23)$$

Let us now consider the fixed point limit of the web diagram for $SU(4)_0 + 4F$

$$(2.24)$$

The magnetic quivers for this brane system are

$$(2.25)$$

The unrefined Coulomb branch and Higgs branch Hilbert series for the orthosymplectic quivers in (2.21) and (2.23) match with their corresponding unitary quivers in (2.25) and are given in table 3 and table 4 respectively. Moreover, we know the HWG of the Coulomb branch of the two cones of (2.25) as

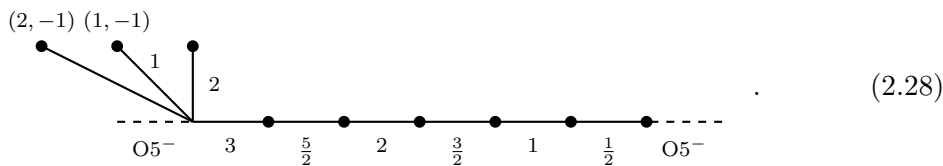
$$\begin{aligned} \text{HWG}_C^1(2.25) &= \text{PE}[t^2(1 + \mu_1\mu_3) + t^4(\mu_2^2 + q_1\mu_2 + q_1^{-1}\mu_2) - t^8\mu_2^2] \\ \text{HWG}_C^2(2.25) &= \text{PE}[t^2 + t^4(q_2 + q_2^{-1}) - t^8], \end{aligned} \quad (2.26)$$

where μ_i are the highest weight fugacities of $SU(4)$ and q_1 and q_2 are $U(1)$ charges. Thus, we can write the HWG for the orthosymplectic quivers as:

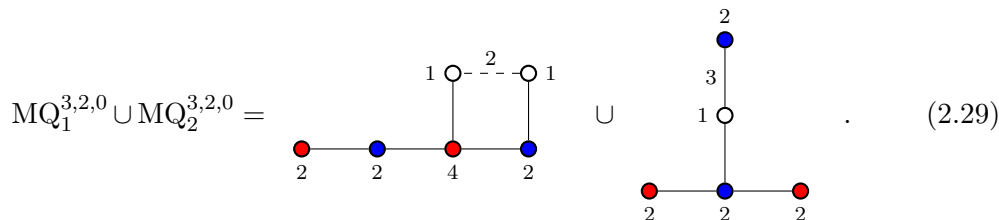
$$\begin{aligned} \text{HWG}_C(\widehat{MQ}_1^{2,2,0}) &= \text{HWG}_C(\widehat{MQ}_1^{2,2,0}) = \text{HWG}_C^1(2.25) \\ \text{HWG}_C(\widehat{MQ}_2^{2,2,0}) &= \text{HWG}_C(\widehat{MQ}_2^{2,2,0}) = \text{HWG}_C^2(2.25). \end{aligned} \quad (2.27)$$

2.1.4 $SO(6) + 3S + 2C \longleftrightarrow SU(4)_{\frac{1}{2}} + 5F$

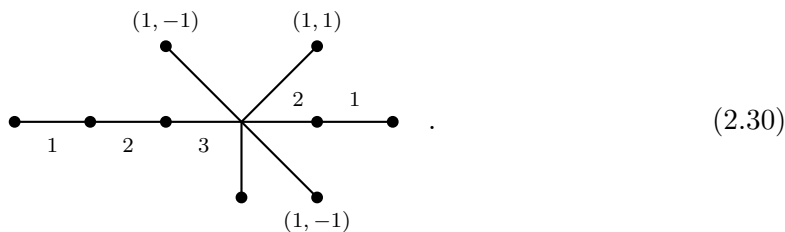
The brane web for $SO(6)+3S+2C$ is given by



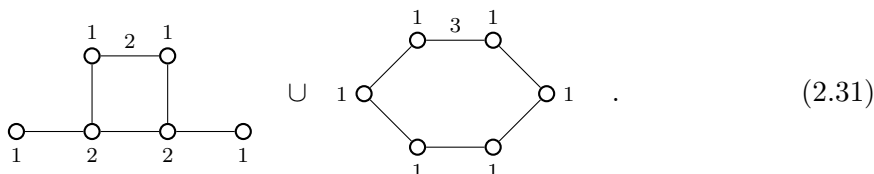
From this brane web we obtain the following magnetic quivers



On the other hand, the brane web for $SU(4)_{\frac{1}{2}}+5F$ is given by



The magnetic quiver one reads off from this ordinary brane web is



The unrefined Coulomb branch and Higgs branch Hilbert series for the orthosymplectic quivers in (2.29) match with their corresponding unitary quivers in (2.31) and are given in table 3 and table 4 respectively. The HWG of the Coulomb branch of the two unitary cones in (2.31) is known by [66]:

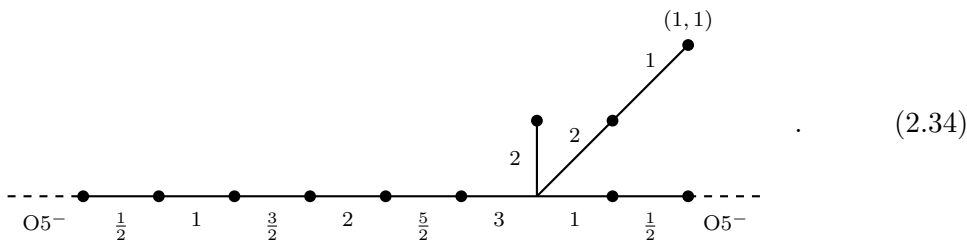
$$\begin{aligned}
 \text{HWG}_{\mathcal{C}}^1(2.31) &= \text{PE} \left[t^2 + (\mu_2 q + \mu_3 q^{-1}) t^4 + \sum_{k=1}^2 \mu_k \mu_{5-k} t^{2k} - \mu_2 \mu_3 t^8 \right], \\
 \text{HWG}_{\mathcal{C}}^2(2.31) &= \text{PE} \left[(1 + \mu_1 \mu_4) t^2 + (\mu_1 q + \mu_4 q^{-1}) t^4 - \mu_1 \mu_4 t^8 \right],
 \end{aligned}
 \tag{2.32}$$

where μ_i are highest weight fugacities of $SU(5)$. Thus from the above discussion, we can conjecture that:

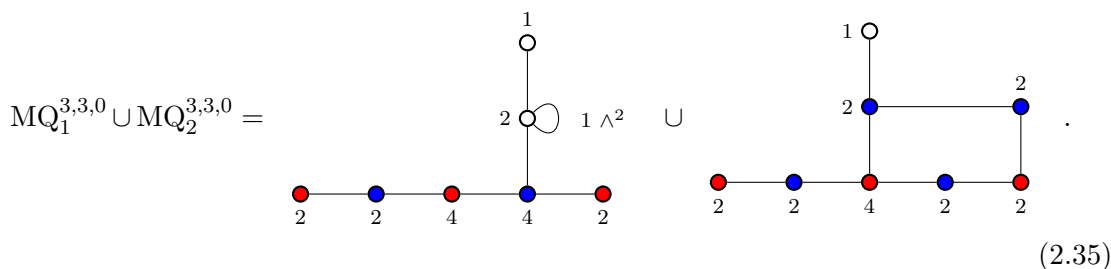
$$\begin{aligned}
 \text{HWG}_{\mathcal{C}}(\text{MQ}_1^{3,2,0}) &= \text{HWG}_{\mathcal{C}}^1(2.31), \\
 \text{HWG}_{\mathcal{C}}(\text{MQ}_2^{3,2,0}) &= \text{HWG}_{\mathcal{C}}^2(2.31).
 \end{aligned}
 \tag{2.33}$$

2.1.5 $SO(6) + 3S + 3C \longleftrightarrow SU(4)_0 + 6F$

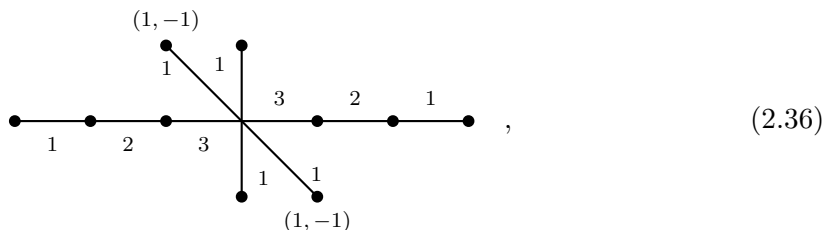
The brane web for $SO(6)+3S+3C$ at infinite coupling is given by



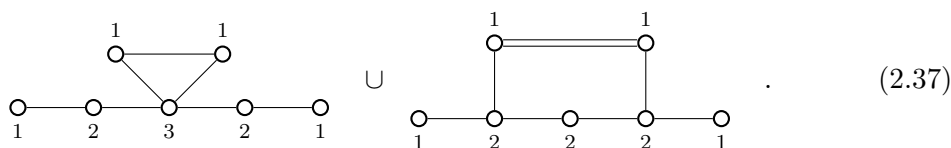
From here we read off the magnetic quiver to be



On the other hand, the brane web for $SU(4)_0+6F$ at infinite coupling is given by



from which we obtain the magnetic quiver



The unrefined Coulomb branch and Higgs branch Hilbert series for the orthosymplectic quivers in (2.35) match with their corresponding unitary quivers in (2.37) and are given in table 3 and table 4 respectively. The HWG of the Coulomb branch of the two cones of (2.37) are given by [66]:

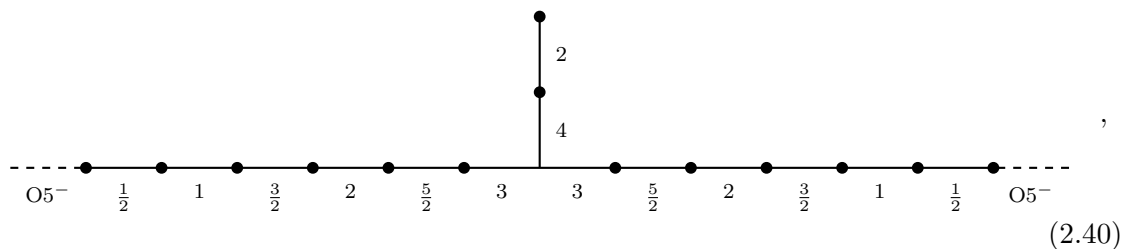
$$\begin{aligned}
 HWG_C^1(2.37) &= PE \left[t^2 + (q + q^{-1})\mu_3 t^4 + \sum_{k=1}^3 \mu_k \mu_{6-k} t^{2k} - \mu_3^2 t^8 \right] \\
 HWG_C^2(2.37) &= PE \left[t^2 + (\mu_4 q + \mu_2 q^{-1}) t^4 + \sum_{k=1}^2 \mu_k \mu_{6-k} t^{2k} - \mu_2 \mu_4 t^8 \right], \quad (2.38)
 \end{aligned}$$

where μ_i are the highest weight fugacities of $SU(6)$. Thus, from the above discussion, we can conjecture that:

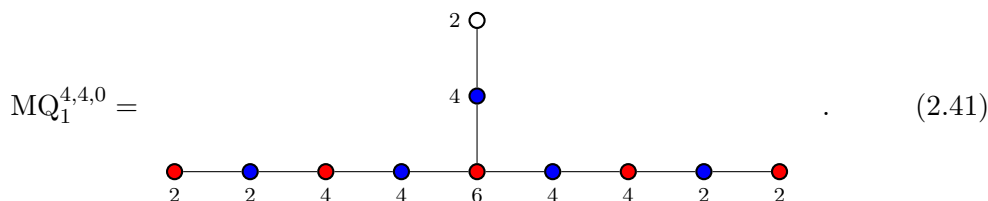
$$\begin{aligned} \text{HWG}_{\mathcal{C}}(\text{MQ}_1^{3,3,0}) &= \text{HWG}_{\mathcal{C}}^1(2.37) \\ \text{HWG}_{\mathcal{C}}(\text{MQ}_2^{3,3,0}) &= \text{HWG}_{\mathcal{C}}^2(2.37). \end{aligned} \quad (2.39)$$

2.1.6 $SO(6) + 4S + 4C \longleftrightarrow SU(4)_0 + 8F$

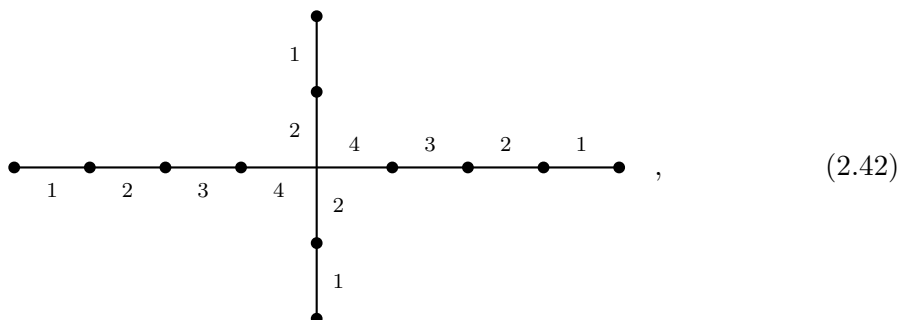
The brane web for $SO(6)+4S+4C$ at infinite coupling is given by



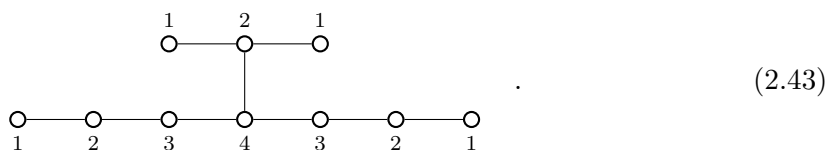
whose corresponding magnetic quiver is



The brane web for $SU(4)_0+8F$ at infinite coupling is given by



from here we obtain the following magnetic quiver



The perturbative results of unrefined Coulomb branch and Higgs branch Hilbert series for the quiver (2.41) match with that of (2.43) and are given in table 3 and table 4 respectively. The HWG of the Coulomb branch of the unitary quiver was computed in [59]. Thus, we can conjecture the following HWG for the orthosymplectic quiver:

$$\text{HWG}_{\mathcal{C}}(\text{MQ}_1^{4,4,0}) = \text{PE} \left[\sum_{i=1}^4 \mu_i \mu_{8-i} t^{2i} + (\nu^2 + \lambda^2) t^2 + t^4 + \mu_4 \nu \lambda (t^4 + t^6) - \nu^2 \lambda^2 \mu_4^2 t^{12} \right], \quad (2.44)$$

where μ_i are $SU(8)$ highest weight fugacities, while ν and λ are $SU(2)$ highest weight fugacities.

2.2 $SO(6)$ theories with a single vector hypermultiplet

We will now begin to examine $SO(6)$ gauge theories with a single hypermultiplet in the vector representation, as well as hypermultiplets in the (conjugate) spinor representations. Accordingly, we will be looking at the magnetic quivers for $SU(4)_\kappa$ gauge theory with a single second rank antisymmetric hypermultiplet, as well as fundamental hypermultiplets. As we shall see, the magnetic quivers do not always have a simple HWG, unlike the previously examined cases. Nevertheless, some magnetic quivers still have a HWG that can be written down in closed form.

2.2.1 $SO(6) + 2S/(1S + 1C) + 1V \longleftrightarrow SU(4)_{1/0} + 2F + 1AS$

Consider $SO(6)$ gauge theory with two spinors or one spinor and a conjugate spinor, in addition to a vector. Both of the theories can be realized by a brane web of the same shape (see the discussion around figure 2) and the brane web at infinite coupling is given by

$$(2, -1) \quad (1, -1) \quad (1, 1) \quad \cdot \quad (2.45)$$

$O5^- \quad 2 \quad \frac{3}{2} \quad O5^-$

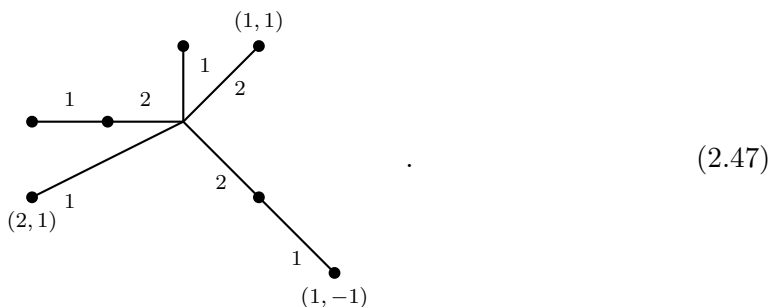
From here we find three subdivisions and the magnetic quivers obtained from the subdivisions are

$$MQ_1^{*,*,1} \cup MQ_2^{*,*,1} \cup MQ_3^{*,*,1} = \text{[Diagram 1]} \cup \text{[Diagram 2]} \cup \text{[Diagram 3]} \quad (2.46)$$

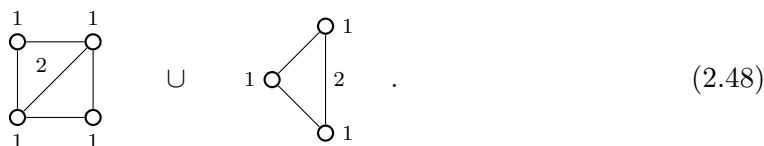
Then a question is which of the magnetic quivers are for $SO(6)+2S+1V$ or $SO(6)+1S+1C+1V$. In section 2.1.1, we encountered a similar situation and at that time some subdivisions corresponded to the magnetic quivers of one theory and the others corresponded to those of the other theory. In this case it turns out that the situation is different due to the presence of bad gauge nodes in the magnetic quivers.

In order to resolve this issue, we consider the magnetic quivers from their unitary counterparts. $SO(6)+1S+1C+1V$ corresponds to $SU(4)_0+2F+1AS$ and its brane web at

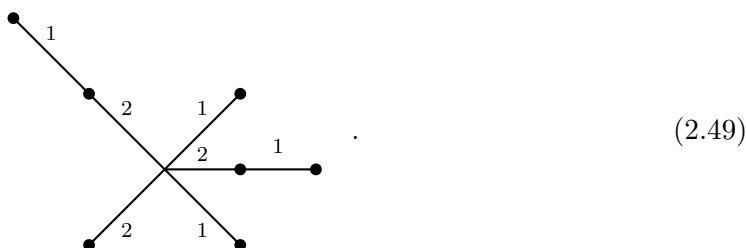
infinite coupling is given by



The diagram admits two subdivisions and the magnetic quivers that one reads off from this brane web are



On the other hand $SO(6)+2\mathbf{S}+1\mathbf{V}$ corresponds to $SU(4)_1+2\mathbf{F}+1\mathbf{AS}$ and its brane web at infinite coupling is given by



This brane web has three subdivisions and the corresponding magnetic quivers are



Hence we have five subdivisions for the two theories in total and the five subdivisions need to fit into the three subdivisions in (2.46).

Among the three magnetic quivers in (2.46), the last quiver $MQ_3^{*,*,1}$ is a good theory and one can compute the Coulomb branch Hilbert series by using the monopole formula. Then it is possible to see that the Hilbert series agrees with that of the rightmost magnetic quiver in (2.50).

When the magnetic quivers contain bad gauge nodes the correspondence could be more involved. In bad theories, the Coulomb branch may not be simply a cone. For example the Coulomb branch of $USp(2N)$ SQCD with $2N$ flavours has two most singular points and the theory flows to an interacting SCFT at low energies at each point [87]. Both the first and the second magnetic quivers in (2.46) contain a bad $USp(2)$ gauge node with 2 effective flavours (which is the $N = 1$ case of aforementioned example), it is natural to

expect that the full Coulomb branch of the bad magnetic quivers is not a single cone. On the other hand, all the magnetic quivers in (2.50) are good theories and so their Coulomb branch is expected to be a single cone. Hence, the Coulomb branch of the first and the second magnetic quivers in (2.46) seem to be different from the magnetic quivers in (2.48) and (2.50).

From the viewpoint of the Higgs branch of 5d theories, we expect that the Higgs branch of 5d $SO(6)+2\mathbf{S}+1\mathbf{V}/SO(6)+1\mathbf{S}+1\mathbf{C}+1\mathbf{V}$ or $SU(4)_1+2\mathbf{F}+1\mathbf{AS}/SU(4)_0+2\mathbf{F}+1\mathbf{AS}$ at the infinite coupling is a union of cones and the origins of the cones are located at the same point where a 5d SCFT is realized. While this picture is consistent with the expectation for the Coulomb branch of the magnetic quivers in (2.48) and (2.50), this does not agree with expectation for the Coulomb branch of the bad magnetic quivers in (2.46). Hence we argue that the Higgs branch of the 5d theories is given by the Coulomb branch of the good unitary quivers in (2.48) and (2.50). As for the bad quivers in (2.46), which contain the bad $USp(2)$ gauge node, we need to extract a part which corresponds to the Coulomb branch of the good unitary quivers from the Coulomb branch of the bad quivers in order to reproduce the Higgs branch of the 5d theories.

We hereby propose a prescription (which we denote as ‘B2G’) that extracts the magnetic quivers whose Coulomb branch agrees with that of the unitary counterparts from magnetic quivers which contain the $USp(2)$ gauge node with two effective flavours. A similar prescription can be given to extract the good magnetic quivers from bad magnetic quivers which contain a $USp(2N)$ gauge node with $2N$ effective flavours. We will discuss more about the $N > 1$ case in an upcoming work [91]. To motivate the prescription, note that the Coulomb branch of the $USp(2)$ gauge theory with two flavours has two most singular points. An SCFT is realized at low energies at each point and it is the same SCFT which arises from the $U(1)$ gauge theory with two flavours [87, 89, 92]. Hence the local geometry in the vicinity of one of the most singular points of the Coulomb branch of $USp(2)+2\mathbf{F}$, which is given by $\mathbb{C}^2/\mathbb{Z}_2$, can be described by the Coulomb branch of $U(1)+2\mathbf{F}$. Then a natural way to change quivers which contain the bad $USp(2)$ gauge nodes into good theories, is to replace the $USp(2)+2\mathbf{F}$ with $U(1)+2\mathbf{F}$. Namely, we use the local geometry near one of the most singular points of the Coulomb branch of $USp(2)+2\mathbf{F}$ to construct the whole Coulomb branch moduli space. In order to embed $U(1)+2\mathbf{F}$ into the original quiver, we need to gauge the flavour symmetry. However we need to be careful of the gauging since the flavour symmetry of $U(1)+2\mathbf{F}$ is different from that of $USp(2)+2\mathbf{F}$. The flavour symmetry of the $USp(2)$ gauge theory with two flavours is $SO(4)$ and either all or a part of the flavour symmetry is gauged in a magnetic quiver. We propose matter contributions to the dimension of the monopole operators in various gaugings. It turns out that there are two ways of implementing the matter contributions which can give different Coulomb branch Hilbert series. We will see that these different Coulomb branch Hilbert series agree with the Coulomb branch Hilbert series of the unitary quivers in (2.48) and (2.50).

When $SO(2)\times SO(2)$ is gauged, the prescription of replacing the bad $USp(2)$ gauge node is given by the following two ways,

$$\dots \text{---} \overset{2}{\bullet} \text{---} \overset{2}{\bullet} \text{---} \overset{2}{\bullet} \text{---} \dots \xrightarrow{\text{B2G}} \dots \text{---} \overset{2}{\bullet} \text{---} \overset{\frac{1}{2}}{\circ} \text{---} \overset{1}{\circ} \text{---} \overset{\frac{1}{2}}{\circ} \text{---} \overset{2}{\bullet} \text{---} \dots \quad , \quad (2.51)$$

or

$$\dots \text{---} \overset{2}{\bullet} \text{---} \overset{2}{\bullet} \text{---} \overset{2}{\bullet} \text{---} \dots \xrightarrow{\mathbf{B2G}} \dots \text{---} \overset{2}{\bullet} \overset{\frac{1}{2}}{\text{---}} \overset{1}{\circ} \overset{\frac{1}{2}}{\text{---}} \overset{2}{\bullet} \text{---} \dots \quad . \quad (2.52)$$

Here the solid/dashed line between SO(2) and U(1), with $\frac{1}{2}$ above it, implies the bifundamental/fundamental-fundamental matter. In the Coulomb branch Hilbert series computations, the contribution to the dimension of the monopole operators from the matter is given by¹

$$\Delta_{\text{hyp}} \left(\overset{2}{\bullet} \overset{\frac{1}{2}}{\text{---}} \overset{1}{\circ} \right) = \frac{1}{2} |m_1 - m_2|, \quad (2.53)$$

$$\Delta_{\text{hyp}} \left(\overset{2}{\bullet} \overset{\frac{1}{2}}{\text{---}} \overset{1}{\circ} \right) = \frac{1}{2} |m_1 + m_2|, \quad (2.54)$$

where m_1 is the magnetic flux for SO(2) and m_2 is the magnetic flux for U(1). Note that this is different from the matter represented by a straight line without $\frac{1}{2}$ between SO(2) and U(1) since in that case U(1) gauge node arises by gauging U(1) part of USp(2). When we consider the local part then the two configurations can be equivalently written as

$$\overset{1}{\circ} \overset{\frac{1}{2}}{\text{---}} \overset{2}{\bullet} = \overset{1}{\circ} \text{---} \overset{1}{\circ}, \quad (2.55)$$

and

$$\overset{1}{\circ} \overset{\frac{1}{2}}{\text{---}} \overset{2}{\bullet} = \overset{1}{\circ} \text{---} \overset{1}{\circ}. \quad (2.56)$$

When SO(3) inside SO(4) is gauged, the prescription is the given by the following replacement,

$$\overset{1}{\bullet} \text{---} \overset{2}{\bullet} \text{---} \overset{3}{\bullet} \text{---} \dots \xrightarrow{\mathbf{B2G}} \overset{1}{\bullet} \overset{\frac{1}{2}}{\text{---}} \overset{1}{\circ} \overset{\frac{1}{2}}{\text{---}} \overset{3}{\bullet} \text{---} \dots \quad . \quad (2.57)$$

Here the contribution from the matter represented by the solid line with $\frac{1}{2}$ on it between U(1) and SO(3) to the dimension of the monopole operators in the Coulomb branch Hilbert series computations is given by:

$$\Delta_{\text{hyp}} \left(\overset{1}{\circ} \overset{\frac{1}{2}}{\text{---}} \overset{3}{\bullet} \right) = \frac{1}{2} |m_1 - m_2| + \frac{1}{4} |m_1|, \quad (2.58)$$

$$\Delta_{\text{hyp}} \left(\overset{1}{\bullet} \overset{\frac{1}{2}}{\text{---}} \overset{1}{\circ} \right) = \frac{1}{4} |m_1|, \quad (2.59)$$

where m_1 is the magnetic flux of U(1) and m_2 is the magnetic flux of SO(3). Finally when the full SO(4) is gauged then the prescription is given by the following replacement,

$$\overset{2}{\bullet} \text{---} \overset{4}{\bullet} \text{---} \dots \xrightarrow{\mathbf{B2G}} \overset{1}{\circ} \overset{\frac{1}{2}}{\text{---}} \overset{4}{\bullet} \text{---} \dots \quad , \quad (2.60)$$

or

$$\overset{2}{\bullet} \text{---} \overset{4}{\bullet} \text{---} \dots \xrightarrow{\mathbf{B2G}} \overset{1}{\circ} \overset{\frac{1}{2}}{\text{---}} \overset{4}{\bullet} \text{---} \dots \quad . \quad (2.61)$$

¹Appropriate modifications are required while using the Molien-Weyl integral to compute the Higgs branch Hilbert series. We do not give explicit expressions, but it should be implicit from the expression of the conformal dimension of the monopole operators.

The contribution from the matter represented by the solid/dashed line between U(1) and SO(4) with $\frac{1}{2}$ on it, to the dimension of the monopole operators in the Coulomb branch Hilbert series computations is given by (see footnote 1):

$$\Delta_{\text{hyp}} \left(\begin{array}{c} 1 \quad \frac{1}{2} \quad 4 \\ \circ \text{---} \bullet \end{array} \right) = \frac{1}{2} (|m_1 - m_{2,1}| + |m_1 - m_{2,2}|), \quad (2.62)$$

$$\Delta_{\text{hyp}} \left(\begin{array}{c} 1 \quad \frac{1}{2} \quad 4 \\ \circ \text{---} \bullet \end{array} \right) = \frac{1}{2} (|m_1 - m_{2,1}| + |m_1 + m_{2,2}|), \quad (2.63)$$

where m_1 is the magnetic flux of U(1) and $m_{2,1}, m_{2,2}$ is the magnetic flux of SO(4).

We can apply the above prescription to the first and second magnetic quivers of (2.46). Each quiver gives rise to two magnetic quivers whether we use the replacement (2.51) or (2.52). From the explicit evaluation of the Hilbert series of the moduli spaces, we find that the replacement (2.51) corresponds to the magnetic quivers of (2.50) and the replacement (2.52) corresponds to the magnetic quivers of (2.48). Namely the correspondence is given by

$$\text{MQ}_1^{2,0,1} \cup \text{MQ}_2^{2,0,1} \cup \text{MQ}_3^{2,0,1} = \begin{array}{c} \text{Diagram 1} \cup \text{Diagram 2} \cup \text{Diagram 3} \end{array}, \quad (2.64)$$

$$\text{MQ}_1^{1,1,1} \cup \text{MQ}_2^{1,1,1} = \begin{array}{c} \text{Diagram 1} \cup \text{Diagram 2} \end{array}. \quad (2.65)$$

We have explicitly computed the unrefined Coulomb branch Hilbert series of the orthosymplectic quivers and they agree with their unitary counterparts. The results are given in table 3. Moreover, since we know the HWG of the Coulomb branch of some of the unitary quivers [66, 79], we can conjecture the same for the orthosymplectic quivers:

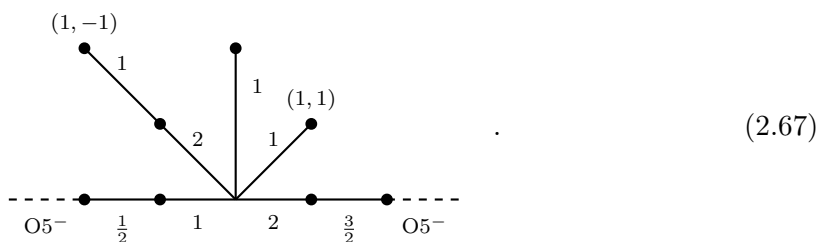
$$\begin{aligned} \text{HWG}_{\mathcal{C}}(\text{MQ}_2^{2,0,1}) &= \text{HWG}_{\mathcal{C}}^2(2.50) = \text{PE} \left[(\mu^2 + \nu^2) t^2 \right] \\ \text{HWG}_{\mathcal{C}}(\text{MQ}_3^{2,0,1}) &= \text{HWG}_{\mathcal{C}}^3(2.50) = \text{PE} \left[(\mu^2 + 1) t^2 + (q + q^{-1}) t^3 - t^6 \right] \\ \text{HWG}_{\mathcal{C}}(\text{MQ}_1^{1,1,1}) &= \text{HWG}_{\mathcal{C}}^1(2.48) = \text{PE} \left[(1 + \mu^2 + \nu^2) t^2 + \mu\nu(q + q^{-1}) t^4 - \mu^2 \nu^2 t^8 \right] \\ \text{HWG}_{\mathcal{C}}(\text{MQ}_2^{1,1,1}) &= \text{HWG}_{\mathcal{C}}^2(2.48) = \text{PE} \left[(1 + \mu^2) t^2 + \mu(q + q^{-1}) t^3 - \mu^2 t^6 \right], \end{aligned} \quad (2.66)$$

where μ and ν are highest weight fugacities of SU(2), and q is the U(1) charge.

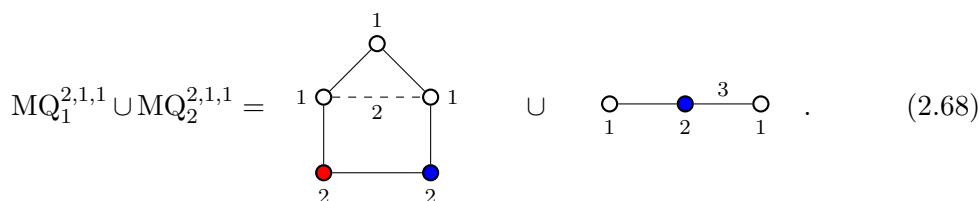
In fact, we found that the same prescription also works for the Higgs branch. The Higgs branch Hilbert series of the magnetic quivers in (2.64) and (2.65) agree with the Higgs branch Hilbert series of the magnetic quivers in (2.50) and (2.48) respectively. The result is summarized in table 4.

2.2.2 $SO(6) + 2S + 1C + 1V \longleftrightarrow SU(4)_{\frac{1}{2}} + 3F + 1AS$

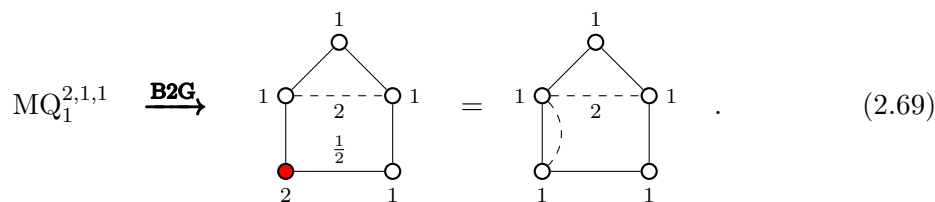
The brane web for $SO(6)+2S+1C+1V$ at infinite coupling is given by



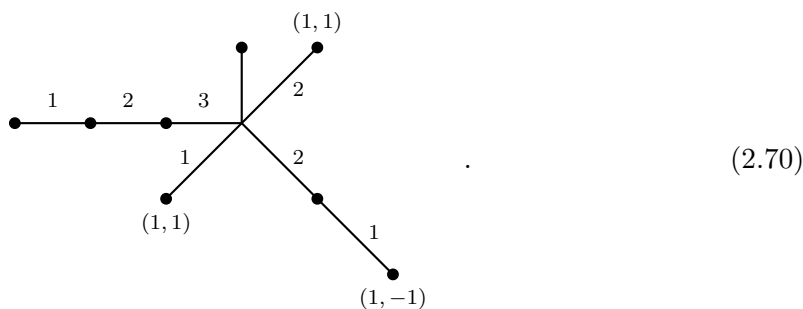
The magnetic quiver extracted from this brane web is



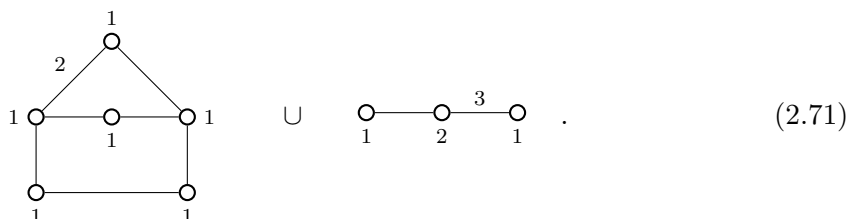
The magnetic quiver $MQ_1^{2,1,1}$ contains a bad $USp(2)$ gauge node and we apply the prescription proposed in section 2.2.1 to extract magnetic quivers which capture the moduli spaces of the unitary counterpart. The magnetic quiver after applying the prescription is given by



Next, consider the brane web for $SU(4)_{\frac{1}{2}}+3F+1AS$



The corresponding unitary magnetic quiver is given by



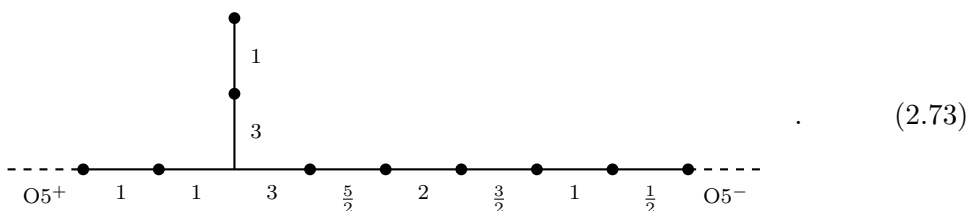
The unrefined Coulomb branch and Higgs branch Hilbert series for the quivers in (2.69) match with the corresponding unitary quivers in (2.71) and are given in table 3 and table 4 respectively. The HWG of the Coulomb branch for the second cone on unitary side is known [93] and so we can write the same for the OSp quiver:

$$\text{HWG}_{\mathcal{C}}(\text{MQ}_2^{2,1,1}) = \text{HWG}_{\mathcal{C}}^2(2.71) = \text{PE} \left[\nu_1 \nu_2 (t^2 + t^4) + (\nu_1^3 + \nu_2^3) t^6 - \nu_1^3 \nu_2^3 t^{12} \right], \quad (2.72)$$

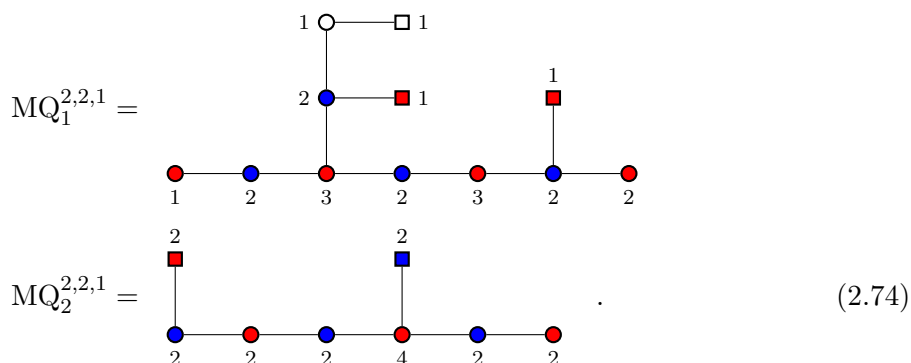
where ν_1 and ν_2 are the highest weight fugacities of SU(3) group.

2.2.3 SO(6) + 2S + 2C + 1V \longleftrightarrow SU(4)₀ + 4F + 1AS

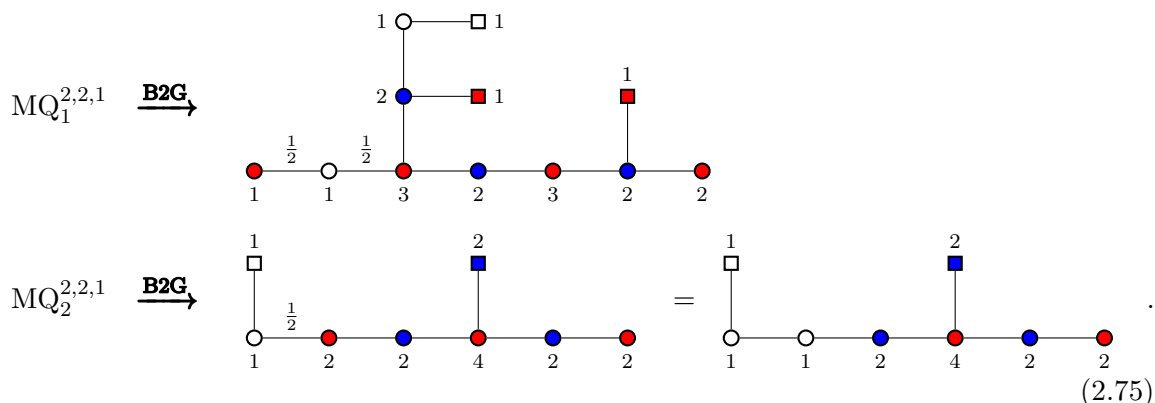
There are two inequivalent web diagrams for SO(6)+2S+2C+1V. The first web diagram, corresponding to the quiver [1V] – SO(6) – [2S + 2C], is given by



The corresponding magnetic quiver for this theory is

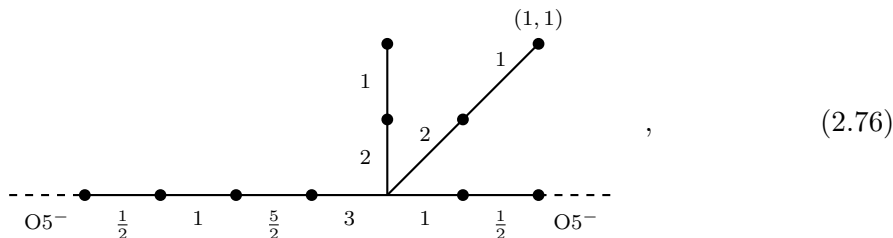


Note that the magnetic quivers $\text{MQ}_1^{2,2,1}$ and $\text{MQ}_2^{2,2,1}$ have a bad USp(2) gauge node. Hence, we use the prescription proposed in section 2.2.1 to extract magnetic quivers which capture the moduli spaces of the unitary counterparts:



An alternative web diagram, for 5d $SO(6)+2\mathbf{S}+2\mathbf{C}+1\mathbf{V}$ can be obtained by considering $[1\mathbf{S} + 1\mathbf{C}] - SO(6) - [1\mathbf{S} + 1\mathbf{C}]$

$$\begin{array}{c} | \\ [1\mathbf{V}] \end{array}$$



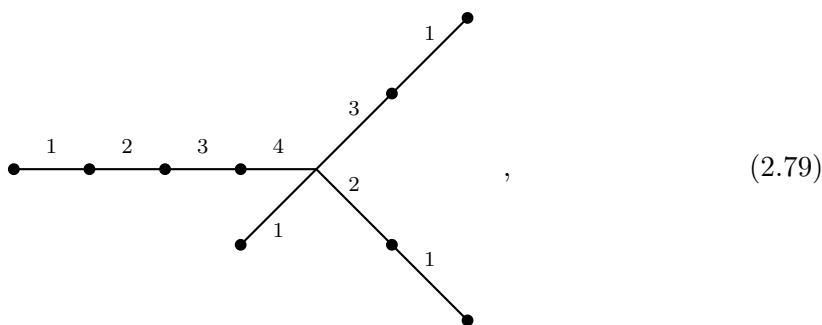
which gives the following magnetic quivers:

$$\widehat{MQ}_1^{2,2,1} = \begin{array}{c} 1 \wedge^2 \\ \circ \quad \circ \\ | \quad | \\ \circ \quad \circ \\ | \quad | \\ \bullet \quad \bullet \\ 2 \quad 4 \quad 2 \end{array} ; \quad \widehat{MQ}_2^{2,2,1} = \begin{array}{c} \circ \quad \circ \\ | \quad | \\ \bullet \quad \bullet \\ | \quad | \\ \bullet \quad \bullet \\ | \quad | \\ \bullet \quad \bullet \end{array} . \quad (2.77)$$

The magnetic quiver $\widehat{MQ}_2^{2,2,1}$ has a bad $USp(2)$ gauge node and we again replace it by a $U(1)$ node using the prescription in section 2.2.1. The magnetic quiver after applying the prescription is given by

$$\widehat{MQ}_2^{2,2,1} \xrightarrow{\mathbf{B2G}} \begin{array}{c} \circ \quad \circ \\ | \quad | \\ \bullet \quad \bullet \\ | \quad | \\ \circ \quad \circ \\ | \quad | \\ \bullet \quad \bullet \\ 1 \quad 2 \end{array} = \begin{array}{c} \circ \quad \circ \\ | \quad | \\ \bullet \quad \bullet \\ | \quad | \\ \circ \quad \circ \\ | \quad | \\ \bullet \quad \bullet \end{array} . \quad (2.78)$$

On the other hand the brane web for $SU(4)_0+4\mathbf{F}+1\mathbf{AS}$ is given as



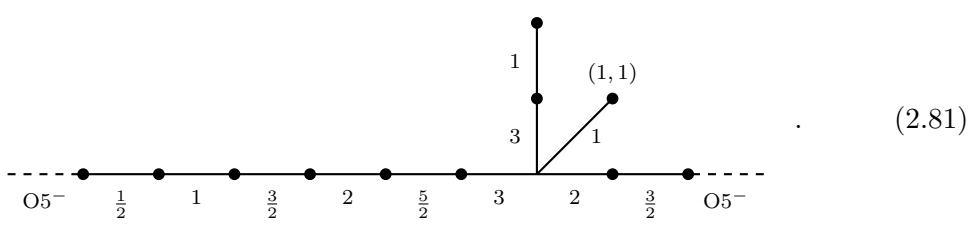
which gives the following two unitary quivers:

$$\begin{array}{c} \circ \quad \circ \quad \circ \\ | \quad | \quad | \\ \circ \quad \circ \quad \circ \\ | \quad | \quad | \\ \circ \quad \circ \quad \circ \\ | \quad | \quad | \\ \circ \quad \circ \quad \circ \end{array} \cup \begin{array}{c} \circ \quad \circ \\ | \quad | \\ \circ \quad \circ \\ | \quad | \\ \circ \quad \circ \\ | \quad | \\ \circ \quad \circ \end{array} . \quad (2.80)$$

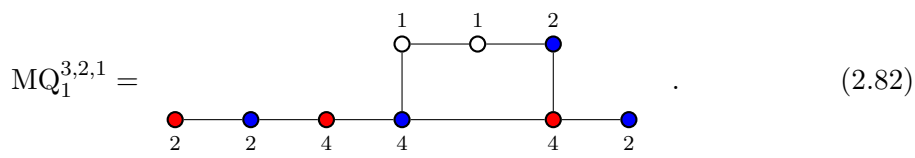
The unrefined Coulomb branch and Higgs branch Hilbert series of the orthosymplectic quivers match with their unitary counterparts and are given in table 3 and table 4 respectively.

2.2.4 $SO(6) + 3S + 2C + 1V \longleftrightarrow SU(4)_{\frac{1}{2}} + 5F + 1AS$

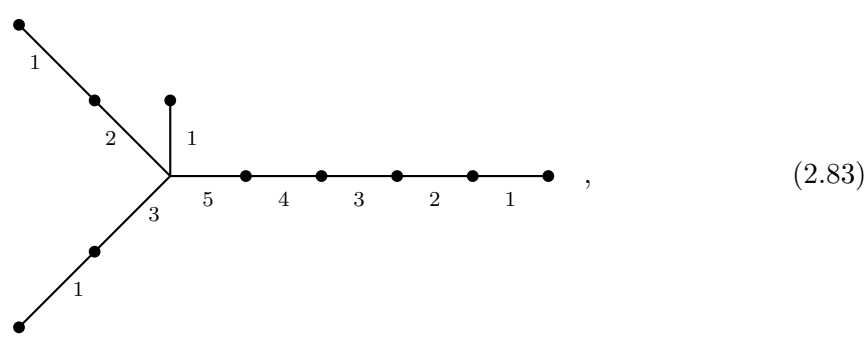
The brane web for the SCFT limit of $SO(6)+3S+2C+1V$ is given by



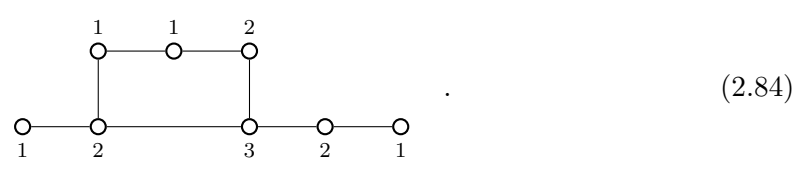
The magnetic quiver associated to this brane system is



On the other hand, the brane web for the SCFT parent of $SU(4)_{\frac{1}{2}}+5F+1AS$ is given by



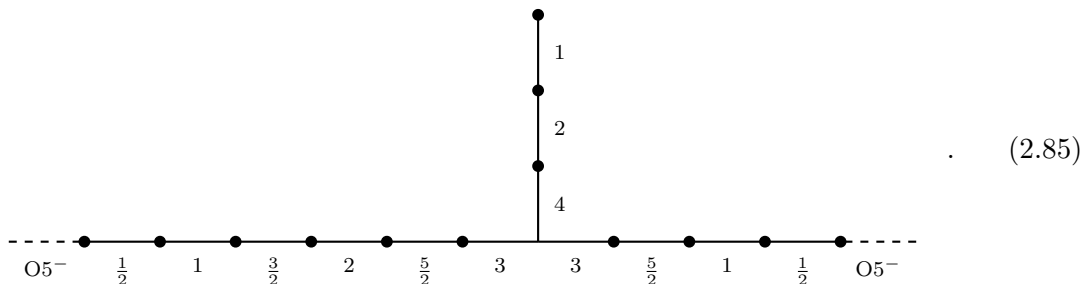
which gives the following unitary quiver:



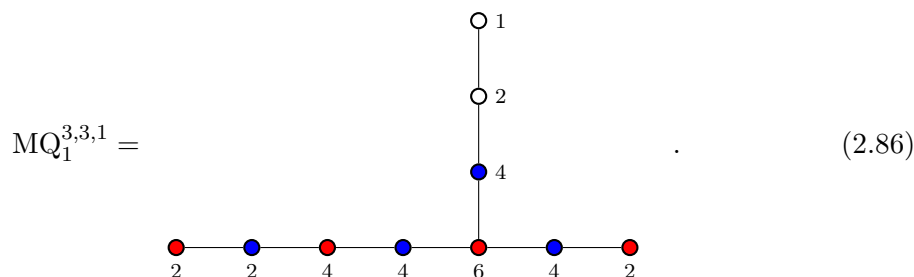
Note that the quiver (2.82) has a bad $USp(2)$ gauge node and we can use our B2G prescription to extract the good quiver. The Coulomb and Higgs branch Hilbert series after doing the B2G replacement agrees with that of the unitary quiver (2.84) and the results are given in table 3 and table 4 respectively.

2.2.5 $SO(6) + 3S + 3C + 1V \longleftrightarrow SU(4)_0 + 6F + 1AS$

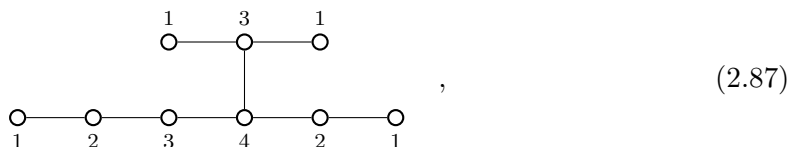
The brane web for $SO(6)+3S+3C+1V$ at infinite coupling is given by



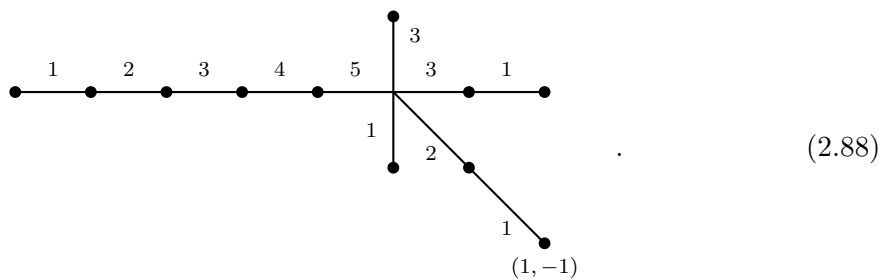
From here we read off the following magnetic quiver



Note that this quiver has a bad $USp(4)$ gauge node. We use our upcoming prescription [91] to compute the Coulomb branch and Higgs branch Hilbert series which are presented in table 3 and table 4 respectively. These Hilbert series are in agreement with the Hilbert series of the following unitary quiver:

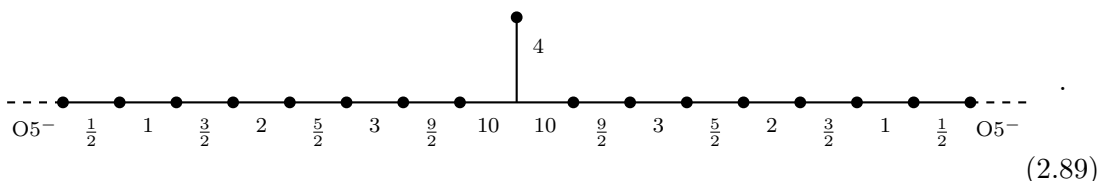


which is associated with the following brane web for $SU(4)_0+6F+1AS$ at infinite coupling:



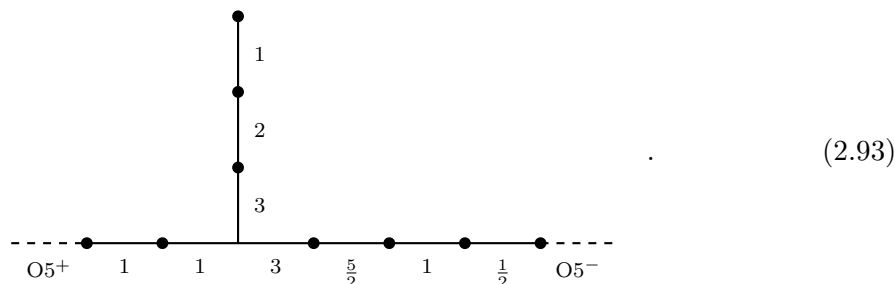
2.2.6 $SO(6) + 4S + 4C + 1V \longleftrightarrow SU(4)_0 + 8F + 1AS$

The brane web for $SO(6)+4S+4C+1V$ at infinite coupling is given by

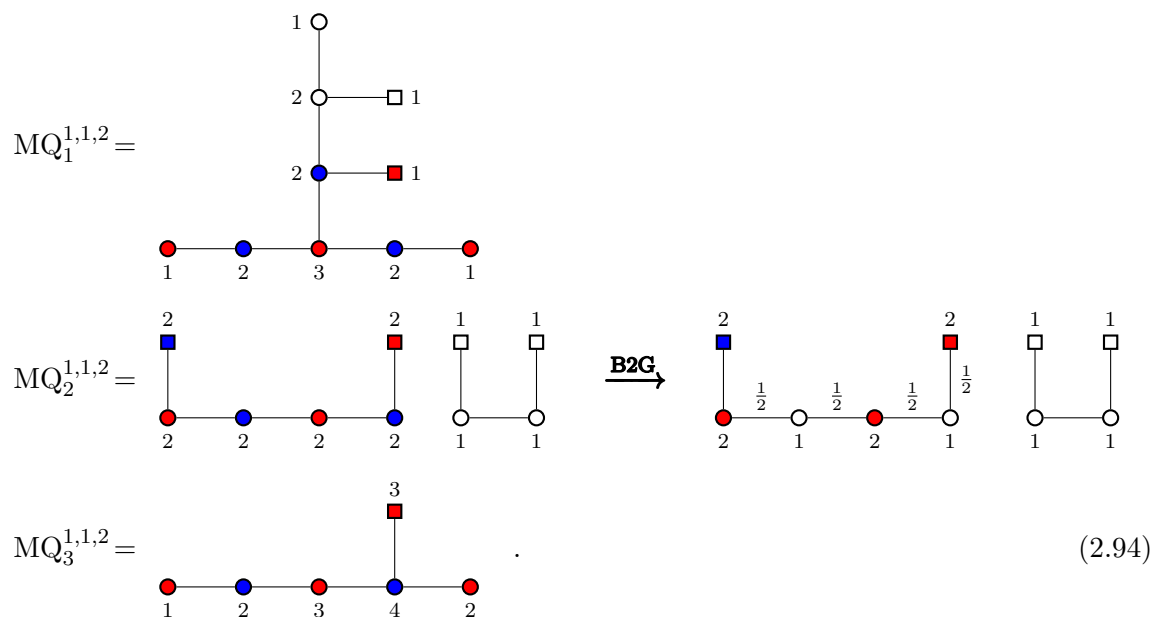


2.3.1 $SO(6) + 2S/(1S + 1C) + 2V \longleftrightarrow SU(4)_{1/0} + 2F + 2AS$

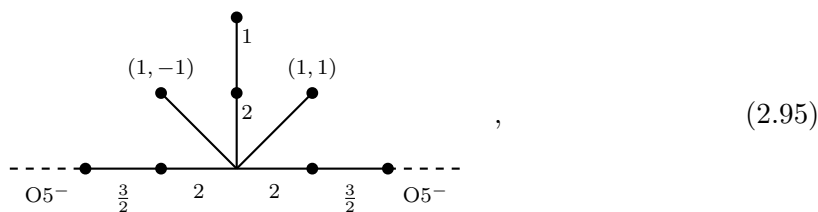
The brane web for $SO(6)+1S+1C+2V$ at infinite coupling is



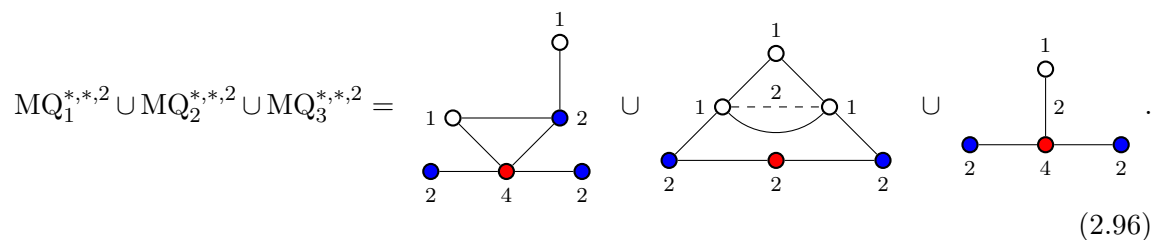
The magnetic quiver for this brane system is given by the union of three cones



We can alternatively consider the brane web for $SO(6)+2S/(1S+1C)+2V$ at infinite coupling



which gives the following magnetic quivers



To distinguish the magnetic quivers for $SO(6)+1\mathbf{S}+1\mathbf{C}+2\mathbf{V}$ from those of $SO(6)+2\mathbf{S}+2\mathbf{V}$, we must apply the B2G procedure to the above magnetic quivers and compare the Hilbert series results with the unitary magnetic quivers for $SU(4)_{0/1}+2\mathbf{F}+2\mathbf{AS}$ (similar to what we did in section 2.2.1). The end result can be summarised as

$$\begin{aligned}
 \widehat{MQ}_1^{1,1,2} &= \text{Diagram 1} & \widehat{MQ}_2^{1,1,2} &= \text{Diagram 2} & \widehat{MQ}_3^{1,1,2} &= \text{Diagram 3} \\
 & & & & & (2.97)
 \end{aligned}$$

$$\begin{aligned}
 MQ_1^{2,0,2} &= \text{Diagram 4} & MQ_2^{2,0,2} &= \text{Diagram 5} & MQ_3^{2,0,2} &= \text{Diagram 6} \\
 & & & & & (2.98)
 \end{aligned}$$

To confirm these results, we can consider the brane web at infinite gauge coupling for $SU(4)_0+2\mathbf{F}+2\mathbf{AS}$

$$\begin{aligned}
 & \text{Diagram 7} \\
 & (2.99)
 \end{aligned}$$

The corresponding magnetic quiver is given by

$$\begin{aligned}
 & \text{Diagram 8} \cup \text{Diagram 9} \cup \text{Diagram 10} \\
 & (2.100)
 \end{aligned}$$

On the other hand the brane web for $SU(4)_1+2\mathbf{F}+2\mathbf{AS}$ at infinite coupling takes the form

(2.101)

whose magnetic quiver is the union of the following three cones

(2.102)

The Coulomb branch and Higgs branch Hilbert series of the quivers in (2.94) and (2.97) match with the corresponding unitary quivers in (2.100), while those of (2.98) match with that of (2.102). The results are given in table 3 and table 4 respectively. Further, the HWG of the Coulomb branch of the second cone in (2.100) is known [66]:

$$\text{HWG}_{\mathcal{C}}^2(2.100) = \text{PE} \left[(1 + \mu_1\mu_3)t^2 + (\mu_1q + \mu_3q^{-1})t^3 - \mu_1\mu_3t^6 \right] \text{PE} \left[\nu_1\nu_2t^2 \right], \quad (2.103)$$

where μ_i and ν_i are the highest weight fugacities associated with the groups $SU(4)$ and $SU(3)$ respectively, and q is the $U(1)$ charge. Thus, the HWG of the Coulomb branch of the corresponding orthosymplectic quivers can be given as:

$$\text{HWG}_{\mathcal{C}}(\text{MQ}_2^{1,1,2}) = \text{HWG}_{\mathcal{C}}(\widehat{\text{MQ}}_2^{1,1,2}) = \text{HWG}_{\mathcal{C}}^2(2.100). \quad (2.104)$$

2.3.2 $SO(6) + 2\mathbf{S} + 1\mathbf{C} + 2\mathbf{V} \longleftrightarrow SU(4)_{\frac{1}{2}} + 3\mathbf{F} + 2\mathbf{AS}$

The brane web for $SO(6)+2\mathbf{S}+1\mathbf{C}+2\mathbf{V}$ at infinite coupling is given by

(2.105)

The magnetic quiver for this brane system is

$$MQ_1^{2,1,2} = \begin{array}{c} \circ_1 \\ | \\ \circ_2 \\ / \quad \backslash \\ \bullet_2 \quad \circ_1 \\ | \quad | \\ \bullet_2 \quad \bullet_4 \quad \bullet_4 \quad \bullet_2 \end{array} . \tag{2.106}$$

Now, let us consider the infinite coupling web diagram for $SU(4)_{\frac{1}{2}}+3\mathbf{F}+2\mathbf{AS}$

$$\begin{array}{c} \bullet \\ | \\ \bullet_1 \\ | \\ \bullet_2 \\ | \\ \bullet \\ / \quad \backslash \\ \bullet_2 \quad \bullet_{(1,1)} \\ | \quad | \\ \bullet_4 \quad \bullet_4 \quad \bullet_2 \\ | \quad | \\ \bullet_2 \quad \bullet_2 \\ | \\ \bullet_{(1,1)} \end{array} , \tag{2.107}$$

which gives the following magnetic quiver:

$$\begin{array}{c} \circ_2 \quad \circ_2 \quad \circ_2 \\ | \quad | \quad | \\ \circ_1 \quad \circ_2 \quad \circ_2 \quad \circ_1 \end{array} . \tag{2.108}$$

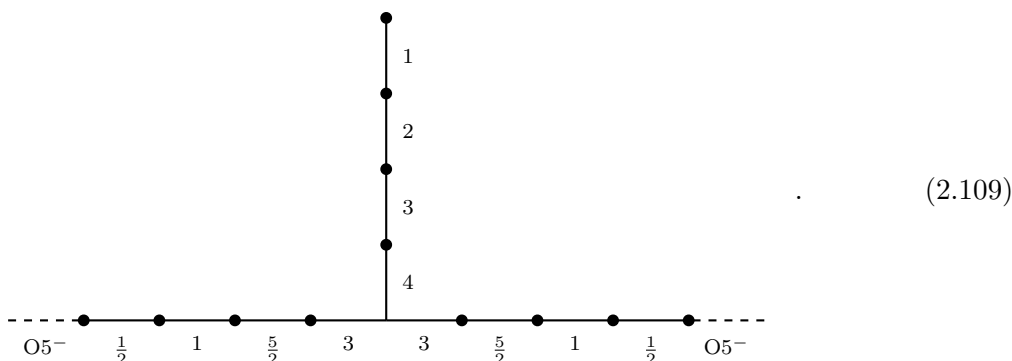
We would like to point out that the quiver in (2.106) has a bad $USp(2)$ and a bad $USp(4)$ node. For the bad $USp(2)$ node, we can use our B2G prescription discussed before. For the bad $USp(4)$ node, we use our upcoming prescription [91] to compute the Coulomb branch and Higgs branch Hilbert series, which are given in table 3 and table 4 respectively. These results are in agreement with that of the unitary quiver in (2.108).

2.3.3 $SO(6) + 2\mathbf{S} + 2\mathbf{C} + 2\mathbf{V} \longleftrightarrow SU(4)_0 + 4\mathbf{F} + 2\mathbf{AS}$

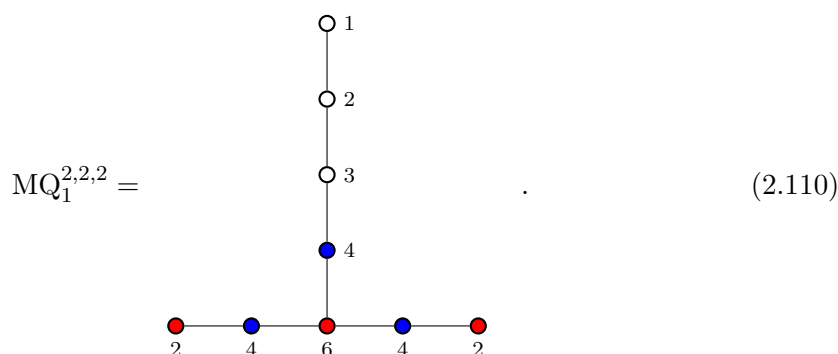
There are two inequivalent web diagrams that engineer the $SO(6)+2\mathbf{S}+2\mathbf{C}+2\mathbf{V}$ theory. The two brane webs differ in their asymptotic $O5$ -plane charges. The first brane configuration, corresponding to the quiver $[1\mathbf{S} + 1\mathbf{C}] - SO(6) - [1\mathbf{S} + 1\mathbf{C}]$ is given at infinite

$$\begin{array}{c} | \\ [2\mathbf{V}] \end{array}$$

coupling by

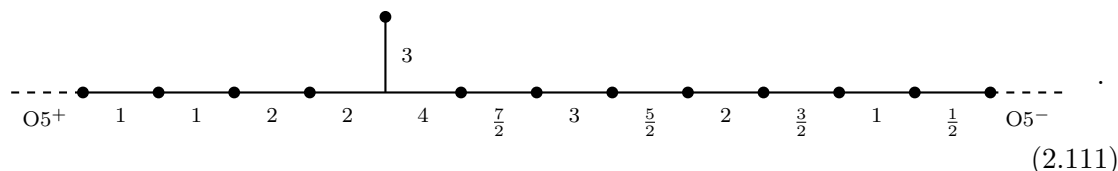


The magnetic quiver one reads from this brane web is

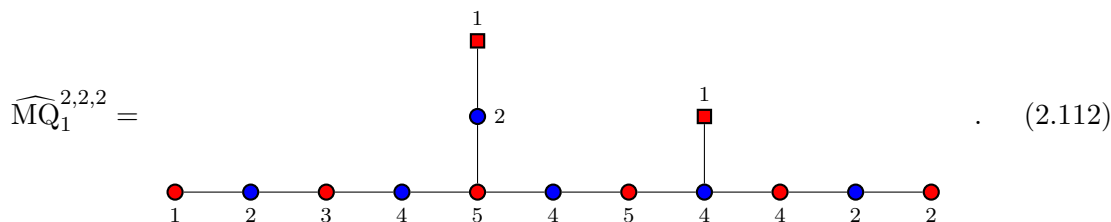


The quiver in (2.110) has two bad $USp(4)$ gauge nodes. We use our upcoming prescription [91] to compute the Coulomb branch and Higgs branch Hilbert series, which are given in table 3 and table 4 respectively.

The second web diagram, realising $SO(6)+2\mathbf{S}+2\mathbf{C}+2\mathbf{V}$, corresponds to the infinite coupling limit of the gauge theory $[2\mathbf{V}] - SO(6) - [2\mathbf{S} + 2\mathbf{C}]$, and is given by

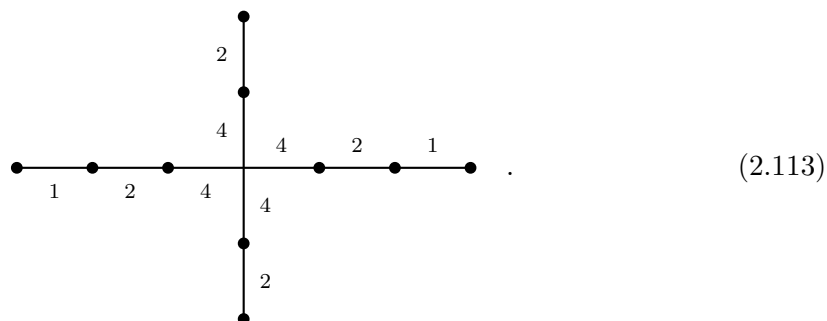


The corresponding magnetic quiver is

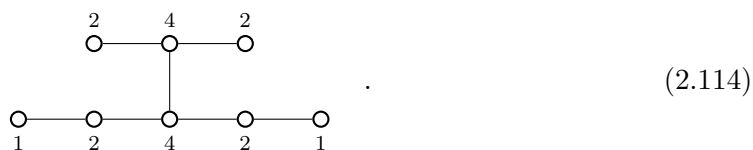


This quiver has a bad $USp(4)$ gauge node and we use upcoming prescription [91] to compute the Coulomb branch and Higgs branch Hilbert series as given in table 3 and table 4 respectively.

Now let us consider the brane web for the infinite gauge coupling limit of $SU(4)_0 + 4F + 2AS$



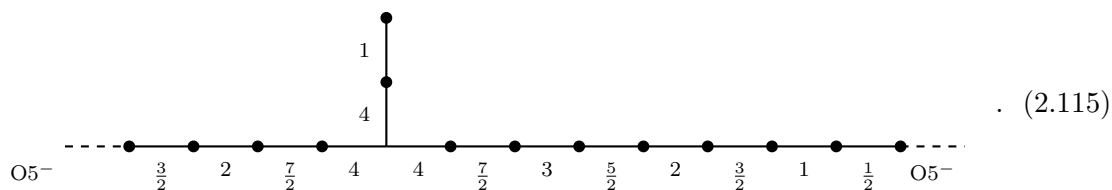
The magnetic quiver for this web diagram is



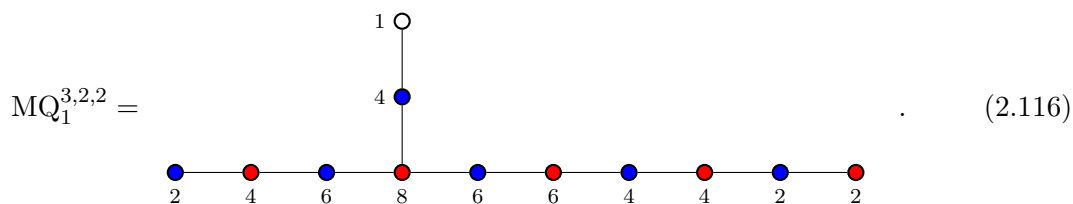
The Hilbert series results of (2.110) and (2.112) mentioned in the appendix match with the Hilbert series results of the quiver (2.114).

2.3.4 $SO(6) + 3S + 2C + 2V \longleftrightarrow SU(4)_{\frac{1}{2}} + 5F + 2AS$

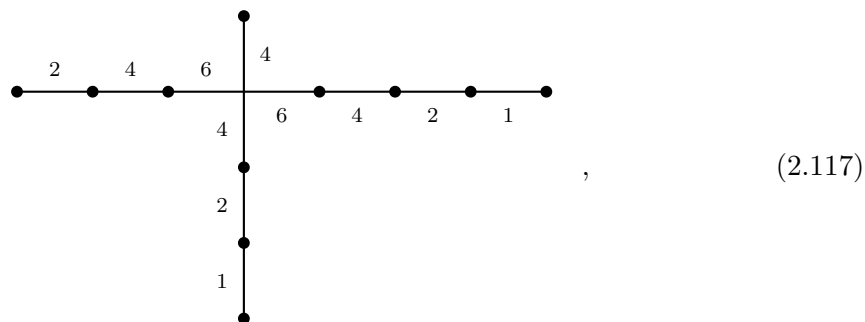
The brane web for the SCFT limit of $SO(6) + 3S + 2C + 2V$ is given by



The magnetic quiver associated to this brane system is given by



If, on the other hand, we consider the brane web for the SCFT limit of $SU(4)_{\frac{1}{2}} + 5F + 2AS$



The magnetic quiver in (2.122) (resp. (2.120)) can also be seen as the 3d mirror of a class-S theory of A_7 (resp. D_5) type on the sphere, with three regular untwisted punctures. The three (Nahm) punctures defining the A -type theory are $[2^3, 1^2]$, $[2^3, 1^2]$, $[4^2]$, while the three (Nahm) punctures defining the D -type theory are $[1^{10}]$, $[2^4, 1^2]$, $[5^2]$. We find for both theories an identical Coulomb branch spectrum given by $\{d_4 = 1, d_5 = 1, d_8 = 1\}$, and identical central charges given by $a = 223/24$ and $c = 65/6$. We take this match as a further evidence for the agreement of the magnetic quivers in (2.122) and (2.120).

Note that the quiver in (2.120) has a bad $USp(4)$ and a bad $USp(8)$ gauge node. We use our upcoming prescription [91] to compute the Coulomb branch and Higgs branch Hilbert series. The perturbative results up to first few orders are given in table 3 and table 4 respectively. These results agree with the Hilbert series of the unitary quiver (2.122).

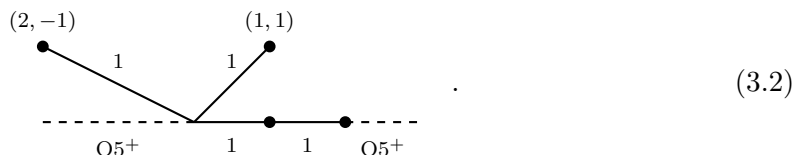
3 SO(8) triality

In this section we consider $SO(8)$ gauge theories with matter in the vector \mathbf{V} , spinor \mathbf{S} and conjugate spinor \mathbf{C} representations. We then use $SO(8)$ triality to produce several equivalent magnetic quivers for a given theory. We will encounter theories whose Higgs branch is given as the union of several cones, where each cone is described by a distinct magnetic quiver. We will denote by $MQ_{i;SO(8)}^{s,c,v}$, the magnetic quiver for the i -th cone of the SCFT parent of $SO(8) + s\mathbf{S} + c\mathbf{C} + v\mathbf{V}$, i.e.

$$\mathcal{H}_{\infty}^{5d}(SO(8) + s\mathbf{S} + c\mathbf{C} + v\mathbf{V}) = \bigcup_i \mathcal{C}^{3d}(MQ_{i;SO(8)}^{s,c,v}). \tag{3.1}$$

3.1 $SO(8) + 1\mathbf{V} \longleftrightarrow SO(8) + 1\mathbf{S}$

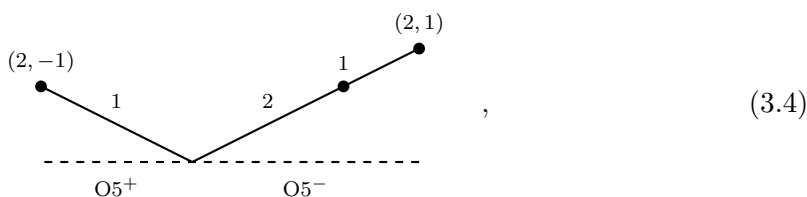
The web diagram for $SO(8)+1\mathbf{V}$ at infinite coupling is given by



The magnetic quiver that we obtain from here is given by

$$MQ_{1;SO(8)}^{0,0,1} = \begin{array}{c} \square_3 \\ | \\ \square_1 \\ \text{---} \\ \square_1 \\ | \\ \square_2 \\ | \\ \square_1 \end{array} \xrightarrow{\text{B2G}} \begin{array}{c} \square_3 \\ | \\ \square_1 \\ \text{---} \\ \square_1 \\ | \\ \square_1 \\ | \\ \square_1 \end{array} = \begin{array}{c} \square_3 \\ | \\ \square_1 \\ \text{---} \\ \square_1 \\ | \\ \square_1 \end{array}. \tag{3.3}$$

On the other hand, the brane web for the infinite coupling limit of $SO(8)+1\mathbf{S}$ is given by



whose magnetic quiver is given by

$$\text{MQ}_{1;\text{SO}(8)}^{1,0,0} = \begin{array}{c} \square \quad \square \\ | \quad | \\ \text{---} \square \text{---} \square \\ | \quad | \\ \square \quad \square \\ 1 \quad 1 \quad 1 \end{array} . \tag{3.5}$$

This coincides with the magnetic quiver obtained in [61] from the brane web with an $O7^+$ -plane. The unrefined Coulomb and Higgs branch Hilbert series of the two quivers agree and are given in table 3 and table 4 respectively. We further propose the following highest weight generating function of the Coulomb branch:

$$\text{HWG}_c(3.3) = \text{HWG}_c(3.5) = \text{PE} \left[\left(1 + \mu^2 \right) t^2 + \left(q + q^{-1} \right) \mu t^6 - \mu^2 t^{12} \right] , \tag{3.6}$$

where μ is the $SU(2)$ fugacity and q is the $U(1)$ charge.

3.2 $SO(8) + 2V \longleftrightarrow SO(8) + 2S$

The web diagram for $SO(8)+2V$ at infinite coupling is given by

$$\begin{array}{c} (1,-1) \quad (1,1) \\ \diagdown \quad \diagup \\ \text{---} \bullet \text{---} \bullet \text{---} \bullet \text{---} \bullet \text{---} \bullet \text{---} \text{---} \\ | \quad | \quad | \quad | \quad | \\ O5^+ \quad 1 \quad 1 \quad 1 \quad 1 \quad O5^+ \end{array} , \tag{3.7}$$

and the corresponding magnetic quiver is given by

$$\text{MQ}_{1;\text{SO}(8)}^{0,0,2} = \begin{array}{c} \square \\ | \\ \text{---} \square \text{---} \square \text{---} \square \text{---} \square \text{---} \square \text{---} \\ | \quad | \quad | \quad | \quad | \\ \bullet \quad \bullet \quad \bullet \quad \bullet \quad \bullet \\ 1 \quad 2 \quad 3 \quad 2 \quad 1 \end{array} . \tag{3.8}$$

By $SO(8)$ triality, the 5d theory $SO(8)+2V$ should be identical to $SO(8)+2S$, the latter has a web at infinite coupling given by

$$\begin{array}{c} (2,-1) \quad (2,1) \\ \diagdown \quad \diagup \\ \text{---} \bullet \text{---} \bullet \text{---} \bullet \text{---} \bullet \text{---} \bullet \text{---} \text{---} \\ | \quad | \quad | \quad | \quad | \\ O5^- \quad 1 \quad 2 \quad 2 \quad 1 \quad O5^- \end{array} . \tag{3.9}$$

Here, we encounter a 5-brane web diagram that includes more than one coincident subwebs that intersect with $O5$ -plane. In this case, we need to consider the two types of contribution: one is the contribution coming from one of the subweb and its mirror image, which corresponds to the factor $|2m_i|$ in the monopole formula. The other is the contribution coming from the mirror pair of different subwebs among coincident ones, which corresponds

to the factor $|m_i + m_j|$ ($i < j$) in the monopole formula. As discussed in [60], the number of each contribution is given by

$$\begin{aligned} \# \text{ of } |2m_i| &: \frac{1}{2}(\text{Self SI}) - (\text{SI with O5}), \\ \# \text{ of } |m_i + m_j| &: (\text{Self SI}) \quad (i < j). \end{aligned} \tag{3.10}$$

Here, ‘‘SI’’ denotes the stable intersection number, which is used to compute the number of hypermultiplets, and ‘‘Self SI’’ means the SI with the mirror images of the considered subwebs.

Both types of contributions need to be part of the weight of representations of the unitary group. Such weights are included in two representations: one is in rank 2 symmetric tensor representation, which we denote as ‘‘Sym²’’, and the other is in rank 2 antisymmetric tensor, which we denote as ‘‘ \wedge^2 ’’. The weight $|2m_i|$ is included only in Sym² while the weight $|m_i + m_j|$ is included in both of the representations. In order to reproduce the contribution mentioned above, we claim that the number of these hypermultiplets are given by

$$\begin{aligned} \# \text{ of Sym}^2 &: \frac{1}{2}(\text{Self SI}) - (\text{SI with O5}), \\ \# \text{ of } \wedge^2 &: \frac{1}{2}(\text{Self SI}) + (\text{SI with O5}). \end{aligned} \tag{3.11}$$

Note that ‘‘Sym²’’ is interpreted as the charge 2 hypermultiplets when the gauge group is U(1). Indeed, the proposal for Sym² above is the generalization of the rule proposed in [60] regarding the number of the charge 2 hypermultiplets. Also, it was proposed in [60] that the number of \wedge^2 is simply given by Self SI, which now turned out to be valid only when the number of Sym² is 0. For generic case, we need to modify the rule as mentioned above.

If we apply this proposal to coincident (p, q) 5-branes intersecting with O5⁻-plane, we have

$$\begin{aligned} \# \text{ of Sym}^2 &: pq - q, \\ \# \text{ of } \wedge^2 &: pq + q. \end{aligned} \tag{3.12}$$

By using this, we claim that the magnetic quiver for the SCFT limit of SO(8)+2S is given by

$$\text{MQ}_{1; \text{SO}(8)}^{2,0,0} = \begin{array}{c} \begin{array}{c} \square \\ | \\ \text{Sym}^2 \\ | \\ \circ \\ | \\ \circ \\ | \\ \circ \end{array} \\ \begin{array}{c} 1 \\ 2 \\ 3 \end{array} \end{array} \cdot \tag{3.13}$$

(Note: The diagram shows a central node with a loop labeled 3 \wedge^2 , connected to two nodes labeled 1, and a chain of nodes labeled 1, 2, 3 with a wavy line labeled Sym² between 1 and 2.)

The unrefined Coulomb and Higgs branch Hilbert series of (3.8) and (3.13) match and are given in table 3 and table 4 respectively. We further propose the following highest weight generating function of the Coulomb branch:

$$\text{HWG}_{\mathcal{C}(3.8)} = \text{HWG}_{\mathcal{C}(3.13)} = \text{PE} \left[\left(1 + \mu_1^2\right) t^2 + \mu_2^2 t^4 + \left(q + q^{-1}\right) \mu_2 t^6 - \mu_2^2 t^{12} \right], \tag{3.14}$$

where μ_i are highest weight fugacities for USp(4), and q is the fugacity for U(1).

From here we read off the following magnetic quiver:

$$MQ_{1;SO(8)}^{1,0,2} = \begin{array}{c} \bullet \\ \text{1} \\ | \\ \bullet \\ \text{2} \\ | \\ \bullet \\ \text{3} \\ | \\ \bullet \\ \text{1} \\ | \\ \bullet \\ \text{1} \\ \text{---} \\ \bullet \\ \text{1} \\ | \\ \bullet \\ \text{2} \\ | \\ \square \\ \text{2} \\ | \\ \square \\ \text{1} \\ | \\ \square \\ \text{1} \end{array} . \tag{3.21}$$

The unrefined Coulomb and Higgs branch Hilbert series of (3.16), (3.18) and (3.21) match and are given in table 3 and table 4 respectively. We further propose the following highest weight generating function of the Coulomb branch of these quivers:

$$HWG_C = PE \left[\left(1 + \mu_1^2 + \nu^2\right) t^2 + \mu_2^2 t^4 + \left(q + q^{-1}\right) \mu_2 \nu t^6 - \mu_2^2 \nu^2 t^{12} \right], \tag{3.22}$$

where μ_i are $USp(4)$ highest weight fugacities, ν is an $SU(2)$ highest weight fugacity, and q is the $U(1)$ charge.

3.4 $SO(8) + 2S + 2C \longleftrightarrow SO(8) + 2S + 2V$

The brane web for $SO(8)+2S+2C$ at infinite coupling is given by

$$\begin{array}{c} \bullet \\ \text{2(1,-1)} \\ \diagdown \\ \text{---} \\ \bullet \\ \text{1} \\ \diagup \\ \bullet \\ \text{2(1,1)} \end{array} \tag{3.23}$$

From this, we obtain the following magnetic quiver:

$$MQ_{1;SO(8)}^{2,2,0} = \begin{array}{c} \bullet \\ \text{2} \\ \text{---} \\ \bullet \\ \text{2} \\ \text{---} \\ \bullet \\ \text{4} \\ \text{---} \\ \bullet \\ \text{2} \\ \text{---} \\ \bullet \\ \text{2} \end{array} ; \quad MQ_{2;SO(8)}^{2,2,0} = \begin{array}{c} \bullet \\ \text{2} \\ \text{---} \\ \bullet \\ \text{2} \\ \text{---} \\ \bullet \\ \text{2} \\ \text{---} \\ \bullet \\ \text{2} \end{array} . \tag{3.24}$$

On the other hand, $SO(8)$ triality implies the equivalence of $SO(8)+2S+2C$ with $SO(8)+2S+2V$. The latter theory has a brane web at infinite coupling given by

$$\begin{array}{c} \bullet \\ \text{(1,-1)} \\ \diagdown \\ \bullet \\ \text{1} \\ \diagup \\ \bullet \\ \text{2} \\ \text{---} \\ \bullet \\ \text{2} \\ \text{---} \\ \bullet \\ \text{2} \\ \text{---} \\ \bullet \\ \text{2} \\ \text{---} \\ \bullet \\ \text{2} \\ \text{---} \\ \bullet \\ \text{(1,1)} \\ \diagdown \\ \bullet \\ \text{1} \\ \diagup \\ \bullet \\ \text{2} \end{array} , \tag{3.25}$$

from which we obtain the corresponding magnetic quiver to be

$$\begin{aligned}
 \text{MQ}_{1;\text{SO}(8)}^{2,0,2} &= \begin{array}{c} \text{Diagram 1} \\ \text{Diagram 2} \end{array} \xrightarrow{\text{B2G}} \begin{array}{c} \text{Diagram 3} \\ \text{Diagram 4} \end{array} \\
 \text{MQ}_{2;\text{SO}(8)}^{2,0,2} &= \text{Diagram 5} \quad . \quad (3.26)
 \end{aligned}$$

The unrefined Coulomb and Higgs branch Hilbert series of $\text{MQ}_{i;\text{SO}(8)}^{2,2,0}$ and $\text{MQ}_{i;\text{SO}(8)}^{2,0,2}$ match and are given in table 3 and table 4 respectively. The HWG's of the Coulomb branches for the second cones take a very simple form and are given as

$$\text{HWG}_C(\text{MQ}_{2;\text{SO}(8)}^{2,2,0}) = \text{HWG}_C(\text{MQ}_{2;\text{SO}(8)}^{2,0,2}) = \text{PE} \left[\mu_1^2 t^2 + (\mu_2 + \mu_2^2) t^4 + \mu_1^2 t^6 + \mu_1^2 \mu_2 t^8 - \mu_1^4 \mu_2^2 t^{16} \right], \quad (3.27)$$

where μ_i are $\text{USp}(4)$ highest weight fugacities.

3.5 $\text{SO}(8) + 1\text{S} + 1\text{C} + 2\text{V} \longleftrightarrow \text{SO}(8) + 2\text{S} + 1\text{C} + 1\text{V}$

The brane web for the SCFT limit of $\text{SO}(8)+1\text{S}+1\text{C}+2\text{V}$ is given by

$$\begin{array}{c} \text{Diagram 1} \end{array} \quad . \quad (3.28)$$

The magnetic quivers associated to this brane system are

$$\begin{aligned}
 \text{MQ}_{1;\text{SO}(8)}^{1,1,2} &= \text{Diagram 1} \\
 \text{MQ}_{2;\text{SO}(8)}^{1,1,2} &= \text{Diagram 2} \quad . \quad (3.29)
 \end{aligned}$$

The brane web for the SCFT limit of $\text{SO}(8)+2\text{S}+1\text{C}+1\text{V}$ is given by

$$\begin{array}{c} \text{Diagram 1} \end{array} \quad . \quad (3.30)$$

The magnetic quiver that we read off here is

$$\begin{aligned}
 \text{MQ}_{1;\text{SO}(8)}^{2,1,1} &= \begin{array}{c} \textcircled{1} \\ | \\ \textcircled{2} \text{ } \textcircled{2} \\ | \\ \text{---} \textcircled{2} \text{---} \textcircled{4} \text{---} \textcircled{2} \text{---} \textcircled{2} \end{array} \xrightarrow{\text{B2G}} \begin{array}{c} \textcircled{1} \\ | \\ \textcircled{2} \text{ } \textcircled{2} \\ | \\ \text{---} \textcircled{1} \text{---} \textcircled{\frac{1}{2}} \text{---} \textcircled{4} \text{---} \textcircled{2} \text{---} \textcircled{2} \end{array} \\
 \text{MQ}_{2;\text{SO}(8)}^{2,1,1} &= \begin{array}{c} \textcircled{1} \\ | \\ \text{---} \textcircled{2} \text{---} \textcircled{2} \text{---} \textcircled{2} \end{array} .
 \end{aligned} \tag{3.31}$$

The unrefined Coulomb and Higgs branch Hilbert series of $\text{MQ}_{i;\text{SO}(8)}^{1,1,2}$ and $\text{MQ}_{i;\text{SO}(8)}^{2,1,1}$ match and are given in table 3 and table 4 respectively. The HWG's for the Coulomb branches for the second cones takes a very simple form

$$\text{HWG}_C(\text{MQ}_{2;\text{SO}(8)}^{1,1,2}) = \text{HWG}_C(\text{MQ}_{2;\text{SO}(8)}^{2,1,1}) = \text{PE} \left[\mu_1^2 t^2 + \left(1 + \mu_2 + \mu_2^2 \right) t^4 + \mu_2 t^6 - \mu_2^2 t^{12} \right], \tag{3.32}$$

where the μ_i are $\text{USp}(4)$ highest weight fugacities.

3.6 $\text{SO}(8) + 2\text{S} + 2\text{C} + 1\text{V} \longleftrightarrow \text{SO}(8) + 2\text{S} + 1\text{C} + 2\text{V}$

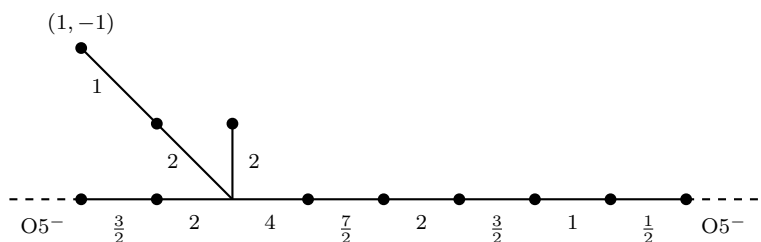
The brane web for the SCFT limit of $\text{SO}(8)+2\text{S}+2\text{C}+1\text{V}$ takes the form

$$\tag{3.33}$$

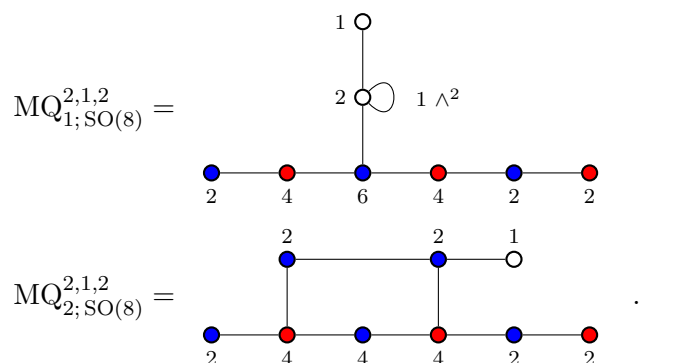
The magnetic quivers associated to this brane system are

$$\begin{aligned}
 \text{MQ}_{1;\text{SO}(8)}^{2,2,1} &= \begin{array}{c} \textcircled{1} \text{ } \textcircled{2} \\ | \\ \textcircled{2} \text{ } \textcircled{2} \\ | \\ \text{---} \textcircled{2} \text{---} \textcircled{2} \text{---} \textcircled{4} \text{---} \textcircled{6} \text{---} \textcircled{4} \text{---} \textcircled{2} \text{---} \textcircled{2} \end{array} \\
 \text{MQ}_{2;\text{SO}(8)}^{2,2,1} &= \begin{array}{c} \textcircled{2} \text{ } \textcircled{2} \\ | \quad | \\ \text{---} \textcircled{2} \text{---} \textcircled{4} \text{---} \textcircled{4} \text{---} \textcircled{4} \text{---} \textcircled{2} \text{---} \textcircled{2} \end{array} .
 \end{aligned} \tag{3.34}$$

If, instead, we take the SCFT limit of the brane web for $SO(8)+2\mathbf{S}+1\mathbf{C}+2\mathbf{V}$, given by


(3.35)

we obtain the following alternative magnetic quivers


(3.36)

The unrefined Coulomb and Higgs branch Hilbert series of $MQ_{i;SO(8)}^{2,2,1}$ and $MQ_{i;SO(8)}^{2,1,2}$ match and are given in table 3 and table 4 respectively.

4 Conclusion

In this paper, we studied the Higgs branches of 5d SCFTs, that admit deformations to $SO(6)$ or $SO(8)$ gauge theories with matter in either the vector, spinor, or conjugate spinor representation of the gauge group. We used the brane configurations, engineering these theories, to find the corresponding magnetic quivers. The magnetic quivers for $SO(6)$ theories were verified by comparison with those of $SU(4)$ theories, while we used $SO(8)$ triality, to provide consistency checks of the magnetic quivers proposed for the $SO(8)$ theories. The agreement of the different magnetic quivers for a given SCFT, were shown to hold at the level of the unrefined Hilbert series, for all cases, on both the Coulomb and the Higgs branch of the moduli space. The unrefined Hilbert series for both the Coulomb and the Higgs branch Hilbert series of all magnetic quivers studied in this work are collected in appendix A. Some magnetic quivers encountered in this work, involved bad symplectic gauge nodes. We were able to assign a Hilbert series for both Coulomb and Higgs branches of these theories, developing a new technique which is referred to as B2G in the main text, which uses a local mirror description of the effective theory around the most singular locus of the moduli space. Details of these computational techniques will be the content of a future publication [91]. Since the Coulomb branch of a bad 3d $\mathcal{N} = 4$ $USp(2N)$ theory is comprised of multiple singular loci, one may wonder whether a 5d Higgs branch whose magnetic quiver contains bad $USp(2N)$ nodes, has a similar structure on its Higgs branch.

However the output of our study seems to suggest otherwise. In particular, we found that for the theories under our construction, the local geometry near one of the two singular points on the Coulomb branch of the magnetic quiver, can capture the full Higgs branch of the 5d theory. This conclusion follows because for every magnetic quiver with a bad node, we have a dual magnetic quiver without any bad nodes. It would be interesting to find further checks of this claim.

We encountered brane webs whose magnetic quivers involve second rank symmetric and second rank antisymmetric tensors. We provided a formula for computing the number of hypermultiplets in the (anti)symmetric representations, which generalises previous rules for extracting magnetic quivers from brane webs with O5-planes in [60, 68]. Despite these improvements, there is still no completely systematic algorithm to extract magnetic quivers for 5d SCFTs engineered using O5-planes. Perhaps the most urgent question to address, is the magnetic quivers for $SO(2r + 1)$ theories, which are engineered using $\widetilde{O5}$ -planes. One might be able to use the results of [62] as a guide for such a study. Another subtle issue, that will eventually need to be addressed, is developing a more systematic method for distinguishing different theories whose 5-brane web at the SCFT limit is identical.

Acknowledgments

We thank Guillermo Arias-Tamargo, Stefano Cremonesi, Julius Grimminger, Amihay Hanany, Alessandro Mininno and Zhenghao Zhong for interesting discussions. SK acknowledges the hospitality at APCTP where part of this work was done. MA is supported by STFC grant ST/S505778/1. F.C. is supported by STFC consolidated grant ST/T000708/1. SD is supported by the NSFC grants No. 12050410249 and No. 11975158. The work of HH is supported in part by JSPS KAKENHI Grant Number JP18K13543. SK and FY are partially supported by the Fundamental Research Funds for the Central Universities 2682021ZTPY043. FY is supported by the NSFC grant No. 11950410490 and by Start-up research grant YH1199911312101.

A Unrefined Hilbert series results for OSp quivers

In this appendix, we collect the unrefined Hilbert series of all the orthosymplectic magnetic quivers appearing in the main sections. The Coulomb branch Hilbert series are given in table 3, while the Higgs branch results are mentioned in table 4. Table 5 contains the palindromic polynomials appearing in table 3 and table 4 respectively.

Quiver	$HS_C(t) = HS_C(t; \vec{m} \in \mathbb{Z}) + HS_C\left(t; \vec{m} \in \mathbb{Z} + \frac{1}{2}\right)$	
	$HS_C(t; \vec{m} \in \mathbb{Z})$	$HS_C\left(t; \vec{m} \in \mathbb{Z} + \frac{1}{2}\right)$
$MQ_1^{1,1,0}$	$\frac{1+3t^4+2t^6+3t^8+t^{12}}{(1-t^2)^2(1-t^4)(1-t^8)}$ \parallel $1 + 2t^2 + 7t^4 + 14t^6 + 29t^8 + 46t^{10} + \dots$	$\frac{2t^2+2t^4+2t^6+2t^8+2t^{10}}{(1-t^2)^2(1-t^4)(1-t^8)}$ \parallel $2t^2 + 6t^4 + 14t^6 + 26t^8 + 46t^{10} + \dots$

Quiver	$\text{HS}_C(t) = \text{HS}_C(t; \vec{m} \in \mathbb{Z}) + \text{HS}_C\left(t; \vec{m} \in \mathbb{Z} + \frac{1}{2}\right)$	
	$\text{HS}_C(t; \vec{m} \in \mathbb{Z})$	$\text{HS}_C\left(t; \vec{m} \in \mathbb{Z} + \frac{1}{2}\right)$
$\text{MQ}_1^{2,0,0}$	$\frac{1+t^4}{(1-t^2)(1-t^4)}$ $1 + t^2 + 3t^4 + 3t^6 + 5t^8 + 5t^{10} + \dots$	not required
$\text{MQ}_2^{2,0,0}$	$\frac{1+t^4}{(1-t^2)(1-t^4)}$ $1 + t^2 + 3t^4 + 3t^6 + 5t^8 + 5t^{10} + \dots$	$\frac{2t^2}{(1-t^2)(1-t^4)}$ $2t^2 + 2t^4 + 4t^6 + 4t^8 + 6t^{10} + \dots$
$\text{MQ}_1^{2,1,0}$	$\frac{P_1(t)}{(1-t^2)^3(1-t^4)^2(1-t^8)}$ $1 + 5t^2 + 24t^4 + 72t^6 + 189t^8 + 413t^{10} + \dots$	$\frac{4t^2 + 6t^4 + 14t^6 + 14t^8 + 14t^{10} + 6t^{12} + 4t^{14}}{(1-t^2)^3(1-t^4)^2(1-t^8)}$ $4t^2 + 18t^4 + 64t^6 + 168t^8 + 388t^{10} + \dots$
$\text{MQ}_1^{2,2,0}$	$\frac{P_2(t)}{(1-t^2)^5(1-t^4)^4(1-t^8)}$ $1 + 8t^2 + 72t^4 + 371t^6 + 1598t^8 + 5510t^{10} + \dots$	$\frac{P_3(t)}{(1-t^2)^5(1-t^4)^4(1-t^8)}$ $8t^2 + 60t^4 + 364t^6 + 1536t^8 + 5464t^{10} + \dots$
$\text{MQ}_2^{2,2,0}$	$\frac{1+t^4}{(1-t^2)(1-t^4)}$ $1 + t^2 + 3t^4 + 3t^6 + 5t^8 + 5t^{10} + \dots$	not required
$\widehat{\text{MQ}}_1^{2,2,0}$	$\frac{P_4(t)}{(1-t^2)^5(1-t^4)^5}$ $1 + 16t^2 + 132t^4 + 735t^6 + 3134t^8 + 10974t^{10} + \dots$	not required
$\widehat{\text{MQ}}_2^{2,2,0}$	$\frac{1+t^4}{(1-t^2)(1-t^4)}$ $1 + t^2 + 3t^4 + 3t^6 + 5t^8 + 5t^{10} + \dots$	not required
$\text{MQ}_1^{3,2,0}$	$1 + 17t^2 + 184t^4 + 1446t^6 + 8758t^8 + 43000t^{10} + 178362t^{12} + 644654t^{14} + 2079047t^{16} + 6092795t^{18} + 16458838t^{20} + \dots$	$8t^2 + 136t^4 + 1248t^6 + 8072t^8 + 40952t^{10} + 172888t^{12} + 631376t^{14} + 2049176t^{16} + 6030000t^{18} + 16333832t^{20} + \dots$
$\text{MQ}_2^{3,2,0}$	$\frac{P_5(t)}{(1-t^2)^5(1-t^4)^4(1-t^8)^4}$ $1 + 17t^2 + 139t^4 + 751t^6 + 3148t^8 + 10894t^{10} + \dots$	$\frac{P_6(t)}{(1-t^2)^5(1-t^4)^4(1-t^8)^4}$ $8t^2 + 96t^4 + 624t^6 + 2832t^8 + 10232t^{10} + \dots$
$\text{MQ}_1^{3,3,0}$	$1 + 20t^2 + 350t^4 + 4199t^6 + 38358t^8 + 278738t^{10} + 1683601t^{12} + 8713628t^{14} + 39600362t^{16} + 161030946t^{18} + 594866176t^{20} + \dots$	$16t^2 + 320t^4 + 4096t^6 + 37920t^8 + 277504t^{10} + 1679744t^{12} + 8704320t^{14} + 39576496t^{16} + 160979760t^{18} + 594751936t^{20} + \dots$
$\text{MQ}_2^{3,3,0}$	$1 + 20t^2 + 340t^4 + 3926t^6 + 33526t^8 + 224534t^{10} + 1240034t^{12} + 5850463t^{14} + 24223718t^{16} + 89832720t^{18} + 303191840t^{20} + \dots$	$16t^2 + 320t^4 + 3872t^6 + 33344t^8 + 224128t^{10} + 1238960t^{12} + 5848352t^{14} + 24218944t^{16} + 89824160t^{18} + 303174592t^{20} + \dots$

Quiver	$HS_C(t) = HS_C(t; \vec{m} \in \mathbb{Z}) + HS_C\left(t; \vec{m} \in \mathbb{Z} + \frac{1}{2}\right)$	
	$HS_C(t; \vec{m} \in \mathbb{Z})$	$HS_C\left(t; \vec{m} \in \mathbb{Z} + \frac{1}{2}\right)$
$MQ_1^{4,4,0}$	$1 + 37t^2 + 1350t^4 + 34389t^6 + 668310t^8 + 10281564t^{10} + 129992857t^{12} + 1388266357t^{14} + 12803207039t^{16} + 103789879656t^{18} + 750444248396t^{20} + \dots$	$32t^2 + 1280t^4 + 34080t^6 + 666016t^8 + 10272864t^{10} + 129948064t^{12} + 1388117408t^{14} + 12802606720t^{16} + 103788095648t^{18} + 750438227104t^{20} + \dots$
$MQ_1^{2,0,1}$	$\frac{P_7(t)}{(1-t^2)^2(1-t^4)(1-t^6)^3}$ $1 + 5t^2 + 18t^4 + 58t^6 + 149t^8 + 325t^{10} + \dots$	$\frac{2t^3 P_8(t)}{(1-t^2)(1-t^4)^2(1-t^6)^3}$ $6t^3 + 26t^5 + 78t^7 + 198t^9 + \dots$
$MQ_2^{2,0,1}$	$\frac{1+t^4}{(1-t^2)^4}$ $1 + 4t^2 + 11t^4 + 24t^6 + 45t^8 + 76t^{10} + \dots$	$\frac{2t^2}{(1-t^2)^4}$ $2t^2 + 8t^4 + 20t^6 + 40t^8 + 70t^{10} + \dots$
$MQ_3^{2,0,1}$	$\frac{1-2t+3t^2-4t^3+6t^4-4t^5+3t^6-2t^7+t^8}{(1-t)^2(1-t^4)(1-t^6)}$ $1 + 2t^2 + 5t^4 + 4t^5 + 10t^6 + 8t^7 + 17t^8 + 16t^9 + 28t^{10} + \dots$	$\frac{2t^2-2t^3+2t^4-2t^5+2t^6}{(1-t)^2(1-t^4)(1-t^6)}$ $2t^2 + 2t^3 + 4t^4 + 4t^5 + 8t^6 + 10t^7 + 16t^8 + 18t^9 + 26t^{10} + \dots$
$MQ_1^{1,1,1}$	$\frac{P_9(t)}{(1-t^2)^3(1-t^4)(1-t^8)^2}$ $1 + 5t^2 + 20t^4 + 60t^6 + 157t^8 + 345t^{10} + \dots$	$\frac{(1-t^4)P_{10}(t)}{(1-t^2)^5(1-t^8)^2}$ $2t^2 + 14t^4 + 50t^6 + 136t^8 + 314t^{10} + \dots$
$MQ_2^{1,1,1}$	$\frac{1+2t^2+2t^4+6t^6+2t^8+2t^{10}+t^{12}}{(1-t^2)^2(1-t^6)^2}$ $1 + 4t^2 + 9t^4 + 22t^6 + 41t^8 + 66t^{10} + \dots$	$\frac{4t^3+4t^5+4t^7+4t^9}{(1-t^2)^2(1-t^6)^2}$ $4t^3 + 12t^5 + 24t^7 + 48t^9 + \dots$
$MQ_1^{2,1,1}$	$1 + 9t^2 + 4t^3 + 57t^4 + 52t^5 + 291t^6 + 312t^7 + 1172t^8 + 1360t^9 + 3932t^{10} + \dots$	$4t^2 + 10t^3 + 36t^4 + 82t^5 + 208t^6 + 426t^7 + 920t^8 + 1708t^9 + 3276t^{10} + \dots$
$MQ_2^{2,1,1}$	$\frac{1+t^2+7t^4+6t^6+7t^8+t^{10}+t^{12}}{(1-t^2)^3(1-t^4)^3}$ $1 + 4t^2 + 19t^4 + 55t^6 + 146t^8 + 317t^{10} + \dots$	$\frac{4t^2+4t^4+8t^6+4t^8+4t^{10}}{(1-t^2)^3(1-t^4)^3}$ $4t^2 + 16t^4 + 56t^6 + 140t^8 + 320t^{10} + \dots$
$MQ_1^{2,2,1}$	$1 + 20t^2 + 28t^3 + 220t^4 + 456t^5 + 1905t^6 + 4132t^7 + 13026t^8 + 27600t^9 + 72438t^{10} + \dots$	not required
$MQ_2^{2,2,1}$	$1 + 19t^2 + 24t^3 + 188t^4 + 368t^5 + 1396t^6 + 2968t^7 + 8302t^8 + 17168t^9 + 40474t^{10} + 79648t^{11} + 167230t^{12} + 312656t^{13} + 603338t^{14} + 1074896t^{15} + 1943919t^{16} + 3316912t^{17} + 5693149t^{18} + 9351600t^{19} + 15372660t^{20} + \dots$	not required
$\widehat{MQ}_1^{2,2,1}$	$1 + 12t^2 + 8t^3 + 124t^4 + 200t^5 + 1033t^6 + 1912t^7 + 6834t^8 + 13192t^9 + 37406t^{10} + \dots$	$8t^2 + 20t^3 + 96t^4 + 256t^5 + 872t^6 + 2220t^7 + 6192t^8 + 14408t^9 + 35032t^{10} + \dots$
$\widehat{MQ}_2^{2,2,1}$	$1 + 11t^2 + 8t^3 + 100t^4 + 176t^5 + 724t^6 + 1448t^7 + 4206t^8 + 8496t^9 + 20394t^{10} + \dots$	$8t^2 + 16t^3 + 88t^4 + 192t^5 + 672t^6 + 1520t^7 + 4096t^8 + 8672t^9 + 20080t^{10} + \dots$

Quiver	$\text{HS}_C(t) = \text{HS}_C(t; \vec{m} \in \mathbb{Z}) + \text{HS}_C\left(t; \vec{m} \in \mathbb{Z} + \frac{1}{2}\right)$	
	$\text{HS}_C(t; \vec{m} \in \mathbb{Z})$	$\text{HS}_C\left(t; \vec{m} \in \mathbb{Z} + \frac{1}{2}\right)$
$\text{MQ}_1^{3,2,1}$	$1 + 21t^2 + 28t^3 + 292t^4 + 710t^5 + 3576t^6 + 10234t^7 + 37720t^8 + 107242t^9 + 331772t^{10} + \dots$	$8t^2 + 24t^3 + 192t^4 + 688t^5 + 2992t^6 + 10144t^7 + 34904t^8 + 106960t^9 + 320096t^{10} + \dots$
$\text{MQ}_1^{3,3,1}$	$1 + 24t^2 + 36t^3 + 497t^4 + 1544t^5 + 9096t^6 + 32876t^7 + 141780t^8 + 501144t^9 + 1831783t^{10} + \dots$	$16t^2 + 48t^3 + 432t^4 + 1648t^5 + 8656t^6 + 33680t^7 + 139248t^8 + 505904t^9 + 1818896t^{10} + \dots$
$\text{MQ}_1^{4,4,1}$	$1 + 46t^2 + 96t^3 + 1836t^4 + 8256t^5 + 66981t^6 + \dots$	$32t^2 + 128t^3 + 1664t^4 + 8704t^5 + 64960t^6 + \dots$
$\text{MQ}_1^{1,1,2}$	$1 + 18t^2 + 205t^4 + 1591t^6 + 9499t^8 + 45959t^{10} + 188535t^{12} + 675381t^{14} + 2163400t^{16} + 6305809t^{18} + 16961842t^{20} + \dots$	not required
$\text{MQ}_2^{1,1,2}$	$1 + 24t^2 + 8t^3 + 255t^4 + 144t^5 + 1716t^6 + 1256t^7 + 8594t^8 + 7312t^9 + 34872t^{10} + 32640t^{11} + 120628t^{12} + 120336t^{13} + 367968t^{14} + 383440t^{15} + 1013621t^{16} + 1088720t^{17} + 2565512t^{18} + 2814744t^{19} + 6045369t^{20} + \dots$	not required
$\text{MQ}_3^{1,1,2}$	$1 + 11t^2 + 8t^3 + 65t^4 + 80t^5 + 295t^6 + 432t^7 + 1122t^8 + 1720t^9 + 3666t^{10} + 5640t^{11} + 10564t^{12} + 16024t^{13} + 27460t^{14} + 40752t^{15} + 65445t^{16} + 94888t^{17} + 144935t^{18} + 205440t^{19} + 301571t^{20} + \dots$	not required
$\widehat{\text{MQ}}_1^{1,1,2}$	$1 + 14t^2 + 129t^4 + 895t^6 + 5071t^8 + 23887t^{10} + 96579t^{12} + 343049t^{14} + 1093344t^{16} + 3176685t^{18} + 8527154t^{20} + \dots$	$4t^2 + 76t^4 + 696t^6 + 4428t^8 + 22072t^{10} + 91956t^{12} + 332332t^{14} + 1070056t^{16} + 3129124t^{18} + 8434688t^{20} + \dots$
$\widehat{\text{MQ}}_2^{1,1,2}$	$1 + 20t^2 + 179t^4 + 32t^5 + 1092t^6 + 416t^7 + 5142t^8 + 2816t^9 + 20024t^{10} + 13600t^{11} + 67328t^{12} + 52544t^{13} + 201208t^{14} + 172576t^{15} + 545849t^{16} + 500352t^{17} + 1365524t^{18} + 1313248t^{19} + 3188473t^{20} + \dots$	$4t^2 + 8t^3 + 76t^4 + 112t^5 + 624t^6 + 840t^7 + 3452t^8 + 4496t^9 + 14848t^{10} + 19040t^{11} + 53300t^{12} + 67792t^{13} + 166760t^{14} + 210864t^{15} + 467772t^{16} + 588368t^{17} + 1199988t^{18} + 1501496t^{19} + 2856896t^{20} + \dots$
$\widehat{\text{MQ}}_3^{1,1,2}$	$1 + 11t^2 + 65t^4 + 295t^6 + 1122t^8 + 3666t^{10} + 10564t^{12} + 27460t^{14} + 65445t^{16} + 144935t^{18} + 301571t^{20} + \dots$	$8t^3 + 80t^5 + 432t^7 + 1720t^9 + 5640t^{11} + 16024t^{13} + 40752t^{15} + 94888t^{17} + 205440t^{19} + \dots$
$\text{MQ}_1^{2,0,2}$	$1 + 14t^2 + 119t^4 + 806t^6 + 4480t^8 + 20886t^{10} + 83778t^{12} + \dots$	$16t^3 + 208t^5 + 1568t^7 + 8736t^9 + 39552t^{11} + \dots$
$\text{MQ}_2^{2,0,2}$	$1 + 20t^2 + 175t^4 + 32t^5 + 1060t^6 + 416t^7 + 4994t^8 + 2784t^9 + 19432t^{10} + 13376t^{11} + 65340t^{12} + 51584t^{13} + 195360t^{14} + 169120t^{15} + 530141t^{16} + 489760t^{17} + 1326692t^{18} + 1284544t^{19} + 3098889t^{20} + \dots$	$2t^2 + 16t^3 + 40t^4 + 208t^5 + 348t^6 + 1408t^7 + 2080t^8 + 6896t^9 + 9640t^{10} + 27184t^{11} + 36784t^{12} + 91248t^{13} + 121040t^{14} + 270672t^{15} + 353936t^{16} + 726832t^{17} + 939242t^{18} + 1797536t^{19} + 2299448t^{20} + \dots$

Quiver	$HS_C(t) = HS_C(t; \vec{m} \in \mathbb{Z}) + HS_C\left(t; \vec{m} \in \mathbb{Z} + \frac{1}{2}\right)$	
	$HS_C(t; \vec{m} \in \mathbb{Z})$	$HS_C\left(t; \vec{m} \in \mathbb{Z} + \frac{1}{2}\right)$
$MQ_3^{2,0,2}$	$1 + 11t^2 + 68t^4 + 313t^6 + 1202t^8 + 3953t^{10} + 11453t^{12} + 29842t^{14} + 71275t^{16} + 158094t^{18} + 329343t^{20} + \dots$	$2t^2 + 32t^4 + 214t^6 + 972t^8 + 3472t^{10} + 10544t^{12} + 28260t^{14} + 68662t^{16} + 153948t^{18} + 323034t^{20} + \dots$
$MQ_1^{2,1,2}$	$1 + 20t^2 + 8t^3 + 275t^4 + 296t^5 + 3045t^6 + 4800t^7 + 27790t^8 + 51128t^9 + 211871t^{10} + \dots$	$6t^2 + 24t^3 + 150t^4 + 504t^5 + 2144t^6 + 6528t^7 + 22284t^8 + 61992t^9 + 182902t^{10} + \dots$
$MQ_1^{2,2,2}$	$1 + 27t^2 + 16t^3 + 537t^4 + 992t^5 + 9266t^6 + 23904t^7 + 133582t^8 + 383712t^9 + 1626798t^{10} + \dots$	$12t^2 + 48t^3 + 384t^4 + 1440t^5 + 7700t^6 + 28192t^7 + 120740t^8 + 417440t^9 + 1536816t^{10} + \dots$
$\widehat{MQ}_1^{2,2,2}$	$1 + 39t^2 + 64t^3 + 921t^4 + 2432t^5 + 16966t^6 + 52096t^7 + 254322t^8 + 801152t^9 + 3163614t^{10} + \dots$	not required
$MQ_1^{3,2,2}$	$1 + 40t^2 + 64t^3 + 1104t^4 + 3520t^5 + 26972t^6 + 108032t^7 + 587528t^8 + 2428480t^9 + 11018073t^{10} + \dots$	$16t^2 + 64t^3 + 736t^4 + 3520t^5 + 22848t^6 + 108032t^7 + 549792t^8 + 2428480t^9 + 10724912t^{10} + \dots$
$MQ_1^{3,3,2}$	$1 + 57t^2 + 88t^3 + 2432t^4 + 9024t^5 + 91715t^6 + \dots$	$32t^2 + 128t^3 + 2016t^4 + 9984t^5 + 85856t^6 + \dots$
$MQ_{1;SO(8)}^{0,0,1}$	$\frac{1+2t^2+2t^4+4t^6+2t^8+2t^{10}+t^{12}}{(1-t^2)^2(1-t^6)^2}$ $1 + 4t^2 + 9t^4 + 20t^6 + 37t^8 + 60t^{10} + \dots$	not required
$MQ_{1;SO(8)}^{1,0,0}$	$\frac{1+2t^2+2t^4+4t^6+2t^8+2t^{10}+t^{12}}{(1-t^2)^2(1-t^6)^2}$ $1 + 4t^2 + 9t^4 + 20t^6 + 37t^8 + 60t^{10} + \dots$	not required
$MQ_{1;SO(8)}^{0,0,2}$	$\frac{P_{11}(t)}{(1-t^2)^4(1-t^6)^4}$ $1 + 11t^2 + 60t^4 + 235t^6 + 745t^8 + 2016t^{10} + \dots$	not required
$MQ_{1;SO(8)}^{2,0,0}$	$\frac{P_{12}(t)}{(1-t^2)^2(1-t^4)^2(1-t^6)^4}$ $1 + 7t^2 + 36t^4 + 133t^6 + 409t^8 + 1082t^{10} + \dots$	$\frac{P_{13}(t)}{(1-t^2)^2(1-t^4)^2(1-t^6)^4}$ $4t^2 + 24t^4 + 102t^6 + 336t^8 + 934t^{10} + \dots$
$MQ_{1;SO(8)}^{2,1,0}$	$1 + 10t^2 + 62t^4 + 291t^6 + 1102t^8 + 3556t^{10} + 10104t^{12} + 25904t^{14} + 60965t^{16} + 133590t^{18} + 275450t^{20} + \dots$	$4t^2 + 36t^4 + 196t^6 + 824t^8 + 2840t^{10} + 8448t^{12} + 22392t^{14} + 54040t^{16} + 120684t^{18} + 252596t^{20} + \dots$
$MQ_{1;SO(8)}^{2,0,1}$	$1 + 10t^2 + 62t^4 + 291t^6 + 1102t^8 + 3556t^{10} + 10104t^{12} + 25904t^{14} + 60965t^{16} + 133590t^{18} + 275450t^{20} + \dots$	$4t^2 + 36t^4 + 196t^6 + 824t^8 + 2840t^{10} + 8448t^{12} + 22392t^{14} + 54040t^{16} + 120684t^{18} + 252596t^{20} + \dots$
$MQ_{1;SO(8)}^{1,0,2}$	$1 + 14t^2 + 98t^4 + 487t^6 + 1926t^8 + 6396t^{10} + 18552t^{12} + 48296t^{14} + 115005t^{16} + 254274t^{18} + 528046t^{20} + \dots$	not required

Quiver	$HS_C(t) = HS_C(t; \vec{m} \in \mathbb{Z}) + HS_C\left(t; \vec{m} \in \mathbb{Z} + \frac{1}{2}\right)$	
	$HS_C(t; \vec{m} \in \mathbb{Z})$	$HS_C\left(t; \vec{m} \in \mathbb{Z} + \frac{1}{2}\right)$
$MQ_{1;SO(8)}^{2,2,0}$	$1 + 13t^2 + 143t^4 + 1106t^6 + 6918t^8 + 35792t^{10} + 159285t^{12} + 623177t^{14} + 2187539t^{16} + 6992878t^{18} + 20617582t^{20} + \dots$	$8t^2 + 104t^4 + 936t^6 + 6200t^8 + 33384t^{10} + 151776t^{12} + 602624t^{14} + 2134800t^{16} + 6868552t^{18} + 20339496t^{20} + \dots$
$MQ_{2;SO(8)}^{2,2,0}$	$1 + 6t^2 + 30t^4 + 110t^6 + 339t^8 + 900t^{10} + 2140t^{12} + 4644t^{14} + 9365t^{16} + 17754t^{18} + 31962t^{20} + \dots$	$4t^2 + 24t^4 + 100t^6 + 320t^8 + 872t^{10} + 2096t^{12} + 4584t^{14} + 9280t^{16} + 17644t^{18} + 31816t^{20} + \dots$
$MQ_{1;SO(8)}^{2,0,2}$	$1 + 17t^2 + 161t^4 + 1178t^6 + 7146t^8 + 36564t^{10} + 161447t^{12} + 628953t^{14} + 2201473t^{16} + 7025402t^{18} + 20688074t^{20} + \dots$	$4t^2 + 86t^4 + 864t^6 + 5972t^8 + 32612t^{10} + 149614t^{12} + 596848t^{14} + 2120866t^{16} + 6836028t^{18} + 20269004t^{20} + \dots$
$MQ_{2;SO(8)}^{2,0,2}$	$1 + 6t^2 + 30t^4 + 110t^6 + 339t^8 + 900t^{10} + 2140t^{12} + 4644t^{14} + 9365t^{16} + 17754t^{18} + 31962t^{20} + \dots$	$4t^2 + 24t^4 + 100t^6 + 320t^8 + 872t^{10} + 2096t^{12} + 4584t^{14} + 9280t^{16} + 17644t^{18} + 31816t^{20} + \dots$
$MQ_{1;SO(8)}^{1,1,2}$	$1 + 17t^2 + 16t^3 + 151t^4 + 248t^5 + 1065t^6 + 2032t^7 + 6375t^8 + 12320t^9 + 32229t^{10} + 61368t^{11} + 140928t^{12} + 261264t^{13} + 545817t^{14} + 978968t^{15} + 1902162t^{16} + 3301248t^{17} + 6048732t^{18} + 10175424t^{19} + 17765022t^{20} + \dots$	not required
$MQ_{2;SO(8)}^{1,1,2}$	$\frac{P_{14}(t)}{(1-t^2)^4(1-t^4)^4}$ $1 + 10t^2 + 55t^4 + 215t^6 + 679t^8 + 1831t^{10} + \dots$	not required
$MQ_{1;SO(8)}^{2,1,1}$	$1 + 13t^2 + 8t^3 + 99t^4 + 124t^5 + 645t^6 + 1016t^7 + 3631t^8 + 6160t^9 + 17605t^{10} + 30684t^{11} + 74988t^{12} + 130632t^{13} + 285329t^{14} + 489484t^{15} + 982434t^{16} + 1650624t^{17} + 3098316t^{18} + 5087712t^{19} + 9046590t^{20} + \dots$	$4t^2 + 8t^3 + 52t^4 + 124t^5 + 420t^6 + 1016t^7 + 2744t^8 + 6160t^9 + 14624t^{10} + 30684t^{11} + 65940t^{12} + 130632t^{13} + 260488t^{14} + 489484t^{15} + 919728t^{16} + 1650624t^{17} + 2950416t^{18} + 5087712t^{19} + 8718432t^{20} + \dots$
$MQ_{2;SO(8)}^{2,1,1}$	$1 + 6t^2 + 31t^4 + 111t^6 + 351t^8 + 927t^{10} + 2222t^{12} + 4811t^{14} + 9745t^{16} + 18463t^{18} + 33309t^{20} + \dots$	$4t^2 + 24t^4 + 104t^6 + 328t^8 + 904t^{10} + 2168t^{12} + 4768t^{14} + 9640t^{16} + 18376t^{18} + 33128t^{20} + \dots$
$MQ_{1;SO(8)}^{2,2,1}$	$1 + 16t^2 + 16t^3 + 192t^4 + 384t^5 + 2037t^6 + 5072t^7 + 19123t^8 + 49824t^9 + 156259t^{10} + \dots$	$8t^2 + 16t^3 + 136t^4 + 384t^5 + 1688t^6 + 5072t^7 + 17400t^8 + 49824t^9 + 148624t^{10} + \dots$
$MQ_{2;SO(8)}^{2,2,1}$	$1 + 15t^2 + 16t^3 + 175t^4 + 368t^5 + 1840t^6 + 4768t^7 + 16982t^8 + 45408t^9 + 135469t^{10} + \dots$	$8t^2 + 16t^3 + 136t^4 + 368t^5 + 1640t^6 + 4768t^7 + 16208t^8 + 45408t^9 + 132744t^{10} + \dots$
$MQ_{1;SO(8)}^{2,1,2}$	$1 + 20t^2 + 16t^3 + 224t^4 + 384t^5 + 2189t^6 + 5072t^7 + 19815t^8 + 49824t^9 + 159015t^{10} + \dots$	$4t^2 + 16t^3 + 104t^4 + 384t^5 + 1536t^6 + 5072t^7 + 16708t^8 + 49824t^9 + 145868t^{10} + \dots$
$MQ_{2;SO(8)}^{2,1,2}$	$1 + 19t^2 + 16t^3 + 211t^4 + 368t^5 + 2020t^6 + 4768t^7 + 17758t^8 + 45408t^9 + 138385t^{10} + \dots$	$4t^2 + 16t^3 + 100t^4 + 368t^5 + 1460t^6 + 4768t^7 + 15432t^8 + 45408t^9 + 129828t^{10} + \dots$

Table 3. Unrefined Coulomb branch Hilbert series for the orthosymplectic quivers.

Quiver	Higgs branch HS: $HS_{\mathcal{H}}(t)$
$MQ_1^{1,1,0}$	$\frac{(1-t)Q_1(t)}{(1-t^2)^4(1-t^3)^3} = 1 + 9t^2 + 6t^3 + 36t^4 + 36t^5 + 112t^6 + 120t^7 + 285t^8 + 320t^9 + 621t^{10} + \dots$
$MQ_1^{2,0,0}$	$\frac{1+9t^2+9t^4+t^6}{(1-t^2)^6} = 1 + 15t^2 + 84t^4 + 300t^6 + 825t^8 + 1911t^{10} + \dots$
$MQ_2^{2,0,0}$	$\frac{1+t^2}{(1-t^2)^2} = 1 + 3t^2 + 5t^4 + 7t^6 + 9t^8 + 11t^{10} + \dots$
$MQ_1^{2,1,0}$	$\frac{Q_2(t)}{(1-t^2)^3(1-t^4)^3} = 1 + 9t^2 + 42t^4 + 136t^6 + 357t^8 + 801t^{10} + \dots$
$MQ_1^{2,2,0}$	$\frac{Q_3(t)}{(1-t^2)(1-t^3)^2(1-t^4)(1-t^5)^2} = 1 + 4t^2 + 4t^3 + 11t^4 + 16t^5 + 31t^6 + 44t^7 + 72t^8 + 104t^9 + 155t^{10} + \dots$
$MQ_2^{2,2,0}$	$\frac{1+9t^2+9t^4+t^6}{(1-t^2)^6} = 1 + 15t^2 + 84t^4 + 300t^6 + 825t^8 + 1911t^{10} + \dots$
$\widehat{MQ}_1^{2,2,0}$	$\frac{Q_3(t)}{(1-t^2)(1-t^3)^2(1-t^4)(1-t^5)^2} = 1 + 4t^2 + 4t^3 + 11t^4 + 16t^5 + 31t^6 + 44t^7 + 72t^8 + 104t^9 + 155t^{10} + \dots$
$\widehat{MQ}_2^{2,2,0}$	$\frac{1+9t^2+9t^4+t^6}{(1-t^2)^6} = 1 + 15t^2 + 84t^4 + 300t^6 + 825t^8 + 1911t^{10} + \dots$
$MQ_1^{3,2,0}$	$\frac{Q_4(t)}{(1-t^2)(1-t^4)^3(1-t^6)^2} = 1 + 4t^2 + 14t^4 + 37t^6 + 86t^8 + 176t^{10} + \dots$
$MQ_2^{3,2,0}$	$\frac{Q_5(t)}{(1-t^2)^3(1-t^6)^3} = 1 + 9t^2 + 36t^4 + 106t^6 + 261t^8 + 561t^{10} + \dots$
$MQ_1^{3,3,0}$	$\frac{(1-t)Q_6(t)}{(1-t^2)(1-t^3)(1-t^4)^2(1-t^5)(1-t^6)(1-t^7)} = 1 + t^2 + 2t^3 + 3t^4 + 4t^5 + 8t^6 + 10t^7 + 15t^8 + 20t^9 + 30t^{10} + \dots$
$MQ_2^{3,3,0}$	$\frac{Q_7(t)}{(1-t^2)(1-t^6)^2(1-t^7)^2(1-t^8)} = 1 + 4t^2 + 10t^4 + 4t^5 + 20t^6 + 16t^7 + 36t^8 + 40t^9 + 67t^{10} + \dots$
$MQ_1^{4,4,0}$	$1 + t^4 + 2t^6 + 5t^8 + 5t^{10} + 12t^{12} + \dots$
$MQ_1^{2,0,1}$	$\frac{(1-t)Q_8(t)}{(1-t^2)^2(1-t^4)^2(1-t^3)^3} = 1 + 5t^2 + 6t^3 + 18t^4 + 26t^5 + 58t^6 + 78t^7 + 149t^8 + 198t^9 + 325t^{10} + \dots$
$MQ_2^{2,0,1}$	$\frac{(1+t^2)^2}{(1-t^2)^4} = 1 + 6t^2 + 19t^4 + 44t^6 + 85t^8 + 146t^{10} + \dots$
$MQ_3^{2,0,1}$	$\frac{1+5t^2+5t^4+t^6}{(1-t^2)^6} = 1 + 11t^2 + 56t^4 + 192t^6 + 517t^8 + 1183t^{10} + \dots$
$MQ_1^{1,1,1}$	$\frac{Q_9(t)}{(1-t)(1-t^2)(1-t^3)^3(1-t^4)} = 1 + 5t^2 + 8t^3 + 16t^4 + 32t^5 + 58t^6 + 88t^7 + 151t^8 + 224t^9 + 329t^{10} + \dots$
$MQ_2^{1,1,1}$	$\frac{1+2t^2+2t^3+2t^4+t^6}{(1-t^2)^2(1-t^3)^2} = 1 + 4t^2 + 4t^3 + 9t^4 + 12t^5 + 22t^6 + 24t^7 + 41t^8 + 48t^9 + 66t^{10} + \dots$
$MQ_1^{2,1,1}$	$\frac{(1-t)Q_{10}(t)}{(1-t^2)^2(1-t^4)^2(1-t^5)^3} = 1 + 5t^2 + 18t^4 + 6t^5 + 46t^6 + 26t^7 + 101t^8 + 78t^9 + 205t^{10} + \dots$
$MQ_2^{2,1,1}$	$\frac{1+2t^2+2t^4+t^6}{(1-t^2)^6} = 1 + 8t^2 + 35t^4 + 111t^6 + 286t^8 + 637t^{10} + \dots$
$MQ_1^{2,2,1}$	$\frac{Q_{11}(t)}{(1-t^4)^2(1-t^5)(1-t^6)^2(1-t^7)} = 1 + t^2 + 2t^3 + 4t^4 + 4t^5 + 9t^6 + 12t^7 + 20t^8 + 26t^9 + 39t^{10} + \dots$
$MQ_2^{2,2,1}$	$\frac{Q_{16}(t)}{(1-t^2)^2(1-t^5)^2(1-t^6)^2} = 1 + 4t^2 + 10t^4 + 4t^5 + 23t^6 + 16t^7 + 46t^8 + 40t^9 + 88t^{10} + \dots$
$\widehat{MQ}_1^{2,2,1}$	$1 + t^2 + 4t^5 + 4t^5 + 9t^6 + 12t^7 + 20t^8 + \dots$

Quiver	Higgs branch HS: $HS_{\mathcal{H}}(t)$
$\widehat{MQ}_2^{2,2,1}$	$\frac{Q_{16}(t)}{(1-t^2)^2(1-t^5)^2(1-t^6)^2} = 1 + 4t^2 + 10t^4 + 4t^5 + 23t^6 + 16t^7 + 46t^8 + 40t^9 + 88t^{10} + \dots$
$MQ_1^{3,2,1}$	$1 + t^2 + 2t^4 + 2t^5 + 4t^6 + 4t^7 + 8t^8 + 8t^9 + 13t^{10} + \dots$
$MQ_1^{3,3,1}$	$1 + t^4 + 2t^6 + 5t^8 + \dots$
$MQ_1^{4,4,1}$	$1 + \mathcal{O}(t^7)$
$MQ_1^{1,1,2}$	$\frac{Q_{12}(t)}{(1-t)(1-t^3)(1-t^4)(1-t^5)^2(1-t^6)} = 1 + t^2 + 2t^3 + 4t^4 + 6t^5 + 10t^6 + 14t^7 + 22t^8 + 32t^9 + 46t^{10} + \dots$
$MQ_2^{1,1,2}$	$\frac{Q_{13}(t)}{(1-t)(1-t^2)^2(1-t^3)(1-t^5)^2} = 1 + 5t^2 + 2t^3 + 14t^4 + 14t^5 + 32t^6 + 44t^7 + 73t^8 + 102t^9 + 157t^{10} + \dots$
$MQ_3^{1,1,2}$	$1 + 3t^2 + 14t^4 + 34t^6 + 89t^8 + \dots$
$\widehat{MQ}_1^{1,1,2}$	$\frac{Q_{12}(t)}{(1-t)(1-t^3)(1-t^4)(1-t^5)^2(1-t^6)} = 1 + t^2 + 2t^3 + 4t^4 + 6t^5 + 10t^6 + 14t^7 + 22t^8 + 32t^9 + 46t^{10} + \dots$
$\widehat{MQ}_2^{1,1,2}$	$\frac{1-t+3t^2-2t^3+4t^4+2t^6+4t^8-2t^9+3t^{10}-t^{11}+t^{12}}{(1-t)(1-t^2)^2(1-t^3)(1-t^5)^2} = 1 + 5t^2 + 2t^3 + 14t^4 + 14t^5 + 32t^6 + 44t^7 + 73t^8 + 102t^9 + 157t^{10} + \dots$
$\widehat{MQ}_3^{1,1,2}$	$\frac{1+5t^4+5t^8+t^{12}}{(1-t^2)^3(1-t^4)^3} = 1 + 3t^2 + 14t^4 + 34t^6 + 89t^8 + 179t^{10} + \dots$
$MQ_1^{2,2,1,2}$	$1 + t^2 + 3t^4 + 2t^5 + 4t^6 + 6t^7 + 8t^8 + \dots$
$MQ_1^{2,2,2}$	$1 + t^4 + 2t^6 + 5t^8 + \dots$
$\widehat{MQ}_1^{2,2,2}$	$1 + t^4 + 2t^6 + 5t^8 + \dots$
$MQ_1^{3,2,2}$	$1 + t^6 + \dots$
$MQ_1^{3,3,2}$	$1 + 2t^2 + 8t^4 + \dots$
$MQ_{1;SO(8)}^{0,0,1}$	$\frac{(1-t)Q_{13}(t)}{(1-t^2)^4(1-t^3)^4(1-t^5)} = 1 + 10t^2 + 18t^3 + 52t^4 + 116t^5 + 250t^6 + 454t^7 + 889t^8 + 1490t^9 + 2538t^{10} + \dots$
$MQ_{1;SO(8)}^{1,0,0}$	$\frac{(1-t)Q_{13}(t)}{(1-t^2)^4(1-t^3)^4(1-t^5)} = 1 + 10t^2 + 18t^3 + 52t^4 + 116t^5 + 250t^6 + 454t^7 + 889t^8 + 1490t^9 + 2538t^{10} + \dots$
$MQ_{1;SO(8)}^{0,0,2}$	$\frac{1+6t^2+27t^4+48t^6+84t^8+86t^{10}+84t^{12}+48t^{14}+27t^{16}+6t^{18}+t^{20}}{(1-t^2)^3(1-t^4)^4(1-t^6)} = 1 + 9t^2 + 55t^4 + 212t^6 + 688t^8 + 1852t^{10} + \dots$
$MQ_{1;SO(8)}^{2,0,0}$	$\frac{1+6t^2+27t^4+48t^6+84t^8+86t^{10}+84t^{12}+48t^{14}+27t^{16}+6t^{18}+t^{20}}{(1-t^2)^3(1-t^4)^4(1-t^6)} = 1 + 9t^2 + 55t^4 + 212t^6 + 688t^8 + 1852t^{10} + \dots$
$MQ_{1;SO(8)}^{2,1,0}$	$1 + 5t^2 + 4t^3 + 25t^4 + 22t^5 + 86t^6 + 86t^7 + 254t^8 + 270t^9 + 648t^{10} + 716t^{11} + 1499t^{12} + 1686t^{13} + 3177t^{14} + \dots$
$MQ_{1;SO(8)}^{2,0,1}$	$\frac{(1-t)Q_{14}(t)}{(1-t^2)^3(1-t^3)^2(1-t^4)^2(1-t^5)(1-t^6)} = 1 + 5t^2 + 4t^3 + 25t^4 + 22t^5 + 86t^6 + 86t^7 + 254t^8 + 270t^9 + 648t^{10} + \dots$
$MQ_{1;SO(8)}^{1,0,2}$	$\frac{(1-t)Q_{14}(t)}{(1-t^2)^3(1-t^3)^2(1-t^4)^2(1-t^5)(1-t^6)} = 1 + 5t^2 + 4t^3 + 25t^4 + 22t^5 + 86t^6 + 86t^7 + 254t^8 + 270t^9 + 648t^{10} + \dots$

Quiver	Higgs branch HS: $HS_{\mathcal{H}}(t)$
$MQ_{1;SO(8)}^{2,2,0}$	$1 + 4t^2 + 11t^4 + 8t^5 + 31t^6 + 32t^7 + 70t^8 + 88t^9 + 170t^{10} + \dots$
$MQ_{2;SO(8)}^{2,2,0}$	$\frac{1+2t^2+2t^4+2t^6+t^8}{(1-t^2)^8} = 1 + 10t^2 + 54t^4 + 210t^6 + 659t^8 + 1772t^{10} + \dots$
$MQ_{1;SO(8)}^{2,0,2}$	$1 + 4t^2 + 11t^4 + 8t^5 + 31t^6 + 32t^7 + 70t^8 + 88t^9 + 170t^{10} + \dots$
$MQ_{2;SO(8)}^{2,0,2}$	$\frac{1+2t^2+2t^4+2t^6+t^8}{(1-t^2)^8} = 1 + 10t^2 + 54t^4 + 210t^6 + 659t^8 + 1772t^{10} + \dots$
$MQ_{1;SO(8)}^{1,1,2}$	$1 + 4t^2 + 10t^4 + 8t^5 + 28t^6 + 28t^7 + 63t^8 + \dots$
$MQ_{2;SO(8)}^{1,1,2}$	$\frac{1+6t^2+17t^4+27t^6+32t^8+27t^{10}+17t^{12}+6t^{14}+t^{16}}{(1-t^2)^4(1-t^4)^4} =$ $1 + 10t^2 + 55t^4 + 215t^6 + 679t^8 + 1831t^{10} + \dots$
$MQ_{1;SO(8)}^{2,1,1}$	$\frac{(1-t)Q_{15}(t)}{(1-t^3)^2(1-t^4)(1-t^5)^3(1-t^6)^2(1-t^8)} =$ $1 + 4t^2 + 10t^4 + 8t^5 + 28t^6 + 28t^7 + 63t^8 + 76t^9 + 148t^{10} + \dots$
$MQ_{2;SO(8)}^{2,1,1}$	$\frac{1+6t^2+17t^4+27t^6+32t^8+27t^{10}+17t^{12}+6t^{14}+t^{16}}{(1-t^2)^4(1-t^4)^4} =$ $1 + 10t^2 + 55t^4 + 215t^6 + 679t^8 + 1831t^{10} + \dots$
$MQ_{1;SO(8)}^{2,2,1}$	$1 + t^2 + 2t^3 + 2t^4 + 2t^5 + 6t^6 + 8t^7 + 13t^8 + \dots$
$MQ_{2;SO(8)}^{2,2,1}$	$1 + 3t^2 + 8t^4 + 2t^5 + 16t^6 + 10t^7 + 32t^8 + \dots$
$MQ_{1;SO(8)}^{2,1,2}$	$1 + t^2 + 2t^3 + 2t^4 + 2t^5 + 6t^6 + 8t^7 + 13t^8 + \dots$
$MQ_{2;SO(8)}^{2,1,2}$	$1 + 3t^2 + 8t^4 + 2t^5 + 16t^6 + 10t^7 + 32t^8 + \dots$

Table 4. Unrefined Higgs branch Hilbert series for the orthosymplectic quivers.

Label	Palindromic Polynomial
$P_1(t)$	$1 + 2t^2 + 10t^4 + 10t^6 + 16t^8 + 10t^{10} + 10t^{12} + 2t^{14} + t^{16}$
$P_2(t)$	$1 + 3t^2 + 38t^4 + 69t^6 + 225t^8 + 240t^{10} + 372t^{12} + 240t^{14} + 225t^{16} + 69t^{18} + 38t^{20} + 3t^{22} + t^{24}$
$P_3(t)$	$8t^2 + 20t^4 + 112t^6 + 156t^8 + 328t^{10} + 276t^{12} + 328t^{14} + 156t^{16} + 112t^{18} + 20t^{20} + 8t^{22}$
$P_4(t)$	$1 + 11t^2 + 57t^4 + 170t^6 + 324t^8 + 398t^{10} + 324t^{12} + 170t^{14} + 57t^{16} + 11t^{18} + t^{20}$
$P_5(t)$	$1 + 12t^2 + 63t^4 + 204t^6 + 550t^8 + 1094t^{10} + 1906t^{12} + 2708t^{14} + 3432t^{16} + 3596t^{18} +$ $3432t^{20} + 2708t^{22} + 1906t^{24} + 1094t^{26} + 550t^{28} + 204t^{30} + 63t^{32} + 12t^{34} + t^{36}$
$P_6(t)$	$8t^2 + 56t^4 + 216t^6 + 536t^8 + 1136t^{10} + 1888t^{12} + 2752t^{14} + 3344t^{16} + 3664t^{18} +$ $3344t^{20} + 2752t^{22} + 1888t^{24} + 1136t^{26} + 536t^{28} + 216t^{30} + 56t^{32} + 8t^{34}$
$P_7(t)$	$1 + 3t^2 + 8t^4 + 21t^6 + 33t^8 + 34t^{10} + 33t^{12} + 21t^{14} + 8t^{16} + 3t^{18} + t^{20}$
$P_8(t)$	$3 + 10t^2 + 20t^4 + 31t^6 + 38t^8 + 31t^{10} + 20t^{12} + 10t^{14} + 3t^{16}$
$P_9(t)$	$1 + 2t^2 + 7t^4 + 12t^6 + 22t^8 + 16t^{10} + 22t^{12} + 12t^{14} + 7t^{16} + 2t^{18} + t^{20}$
$P_{10}(t)$	$2t^2 + 4t^4 + 2t^6 + 10t^8 + 2t^{10} + 4t^{12} + 2t^{14}$
$P_{11}(t)$	$1 + 7t^2 + 22t^4 + 53t^6 + 94t^8 + 129t^{10} + 148t^{12} + 129t^{14} + 94t^{16} + 53t^{18} + 22t^{20} + 7t^{22} + t^{24}$

Label	Palindromic Polynomial
$P_{12}(t)$	$1 + 5t^2 + 21t^4 + 54t^6 + 114t^8 + 182t^{10} + 248t^{12} + 270t^{14} + 248t^{16} + 182t^{18} + 114t^{20} + 54t^{22} + 21t^{24} + 5t^{26} + t^{28}$
$P_{13}(t)$	$4t^2 + 16t^4 + 50t^6 + 108t^8 + 188t^{10} + 252t^{12} + 284t^{14} + 252t^{16} + 188t^{18} + 108t^{20} + 50t^{22} + 16t^{24} + 4t^{26}$
$P_{14}(t)$	$1 + 6t^2 + 17t^4 + 27t^6 + 32t^8 + 27t^{10} + 17t^{12} + 6t^{14} + t^{16}$
$Q_1(t)$	$1 + t + 6t^2 + 9t^3 + 15t^4 + 12t^5 + 15t^6 + 9t^7 + 6t^8 + t^9 + t^{10}$
$Q_2(t)$	$1 + 6t^2 + 15t^4 + 18t^6 + 15t^8 + 6t^{10} + t^{12}$
$Q_3(t)$	$1 + 3t^2 + 2t^3 + 6t^4 + 4t^5 + 10t^6 + 6t^7 + 9t^8 + 6t^9 + 10t^{10} + 4t^{11} + 6t^{12} + 2t^{13} + 3t^{14} + t^{16}$
$Q_4(t)$	$1 + 3t^2 + 7t^4 + 12t^6 + 16t^8 + 16t^{10} + 16t^{12} + 12t^{14} + 7t^{16} + 3t^{18} + t^{20}$
$Q_5(t)$	$1 + 6t^2 + 12t^4 + 21t^6 + 24t^8 + 24t^{10} + 21t^{12} + 12t^{14} + 6t^{16} + t^{18}$
$Q_6(t)$	$1 + t + t^2 + 2t^3 + 2t^4 + 3t^5 + 5t^6 + 6t^7 + 7t^8 + 7t^9 + 7t^{10} + 7t^{11} + 8t^{12} + 7t^{13} + 7t^{14} + 7t^{15} + 7t^{16} + 6t^{17} + 5t^{18} + 3t^{19} + 2t^{20} + 2t^{21} + t^{22} + t^{23} + t^{24}$
$Q_7(t)$	$1 + 3t^2 + 6t^4 + 2t^5 + 10t^6 + 4t^7 + 15t^8 + 6t^9 + 21t^{10} + 8t^{11} + 22t^{12} + 10t^{13} + 25t^{14} + 10t^{15} + 22t^{16} + 8t^{17} + 21t^{18} + 6t^{19} + 15t^{20} + 4t^{21} + 10t^{22} + 2t^{23} + 6t^{24} + 3t^{26} + t^{28}$
$Q_8(t)$	$1 + t + 4t^2 + 7t^3 + 14t^4 + 19t^5 + 25t^6 + 24t^7 + 25t^8 + 19t^9 + 14t^{10} + 7t^{11} + 4t^{12} + t^{13} + t^{14}$
$Q_9(t)$	$1 - t + 4t^2 + t^3 + 5t^4 + 2t^5 + 5t^6 + t^7 + 4t^8 - t^9 + t^{10}$
$Q_{10}(t)$	$1 + t + 4t^2 + 4t^3 + 11t^4 + 14t^5 + 23t^6 + 28t^7 + 38t^8 + 37t^9 + 44t^{10} + 37t^{11} + 38t^{12} + 28t^{13} + 23t^{14} + 14t^{15} + 11t^{16} + 4t^{17} + 4t^{18} + t^{19} + t^{20}$
$Q_{11}(t)$	$1 + t^2 + 2t^3 + 2t^4 + 3t^5 + 5t^6 + 6t^7 + 9t^8 + 11t^9 + 12t^{10} + 13t^{11} + 16t^{12} + 12t^{13} + 16t^{14} + 13t^{15} + 12t^{16} + 11t^{17} + 9t^{18} + 6t^{19} + 5t^{20} + 3t^{21} + 2t^{22} + 2t^{23} + t^{24} + t^{26}$
$Q_{12}(t)$	$1 - t + t^2 + 2t^4 + 3t^6 + t^7 + 2t^8 + t^9 + 2t^{10} + t^{11} + 3t^{12} + 2t^{14} + t^{16} - t^{17} + t^{18}$
$Q_{13}(t)$	$1 + t + 7t^2 + 21t^3 + 39t^4 + 58t^5 + 90t^6 + 110t^7 + 118t^8 + 110t^9 + 90t^{10} + 58t^{11} + 39t^{12} + 21t^{13} + 7t^{14} + t^{15} + t^{16}$
$Q_{14}(t)$	$1 + t + 3t^2 + 5t^3 + 16t^4 + 21t^5 + 34t^6 + 34t^7 + 53t^8 + 56t^9 + 73t^{10} + 64t^{11} + 73t^{12} + 56t^{13} + 53t^{14} + 34t^{15} + 34t^{16} + 21t^{17} + 16t^{18} + 5t^{19} + 3t^{20} + t^{21} + t^{22}$
$Q_{15}(t)$	$1 + t + 5t^2 + 3t^3 + 12t^4 + 9t^5 + 32t^6 + 30t^7 + 68t^8 + 65t^9 + 119t^{10} + 114t^{11} + 187t^{12} + 181t^{13} + 268t^{14} + 248t^{15} + 330t^{16} + 287t^{17} + 354t^{18} + 287t^{19} + 330t^{20} + 248t^{21} + 268t^{22} + 181t^{23} + 187t^{24} + 114t^{25} + 119t^{26} + 65t^{27} + 68t^{28} + 30t^{29} + 32t^{30} + 9t^{31} + 12t^{32} + 3t^{33} + 5t^{34} + t^{35} + t^{36}$
$Q_{16}(t)$	$1 + 2t^2 + 3t^4 + 2t^5 + 5t^6 + 4t^7 + 6t^8 + 6t^9 + 6t^{10} + 6t^{11} + 6t^{12} + 4t^{13} + 5t^{14} + 2t^{15} + 3t^{16} + 2t^{18} + t^{20}$

Table 5. Palindromic polynomials appearing in the main sections.

Open Access. This article is distributed under the terms of the Creative Commons Attribution License ([CC-BY 4.0](https://creativecommons.org/licenses/by/4.0/)), which permits any use, distribution and reproduction in any medium, provided the original author(s) and source are credited.

References

- [1] N. Seiberg, *Five-dimensional SUSY field theories, nontrivial fixed points and string dynamics*, *Phys. Lett. B* **388** (1996) 753 [[hep-th/9608111](#)] [[INSPIRE](#)].
- [2] K.A. Intriligator, D.R. Morrison and N. Seiberg, *Five-dimensional supersymmetric gauge theories and degenerations of Calabi-Yau spaces*, *Nucl. Phys. B* **497** (1997) 56 [[hep-th/9702198](#)] [[INSPIRE](#)].
- [3] O.J. Ganor, D.R. Morrison and N. Seiberg, *Branes, Calabi-Yau spaces, and toroidal compactification of the $N = 1$ six-dimensional E_8 theory*, *Nucl. Phys. B* **487** (1997) 93 [[hep-th/9610251](#)] [[INSPIRE](#)].
- [4] A. Brandhuber and Y. Oz, *The D4–D8 brane system and five-dimensional fixed points*, *Phys. Lett. B* **460** (1999) 307 [[hep-th/9905148](#)] [[INSPIRE](#)].
- [5] O. Aharony, A. Hanany and B. Kol, *Webs of (p, q) five-branes, five-dimensional field theories and grid diagrams*, *JHEP* **01** (1998) 002 [[hep-th/9710116](#)] [[INSPIRE](#)].
- [6] O. Aharony and A. Hanany, *Branes, superpotentials and superconformal fixed points*, *Nucl. Phys. B* **504** (1997) 239 [[hep-th/9704170](#)] [[INSPIRE](#)].
- [7] O. Bergman, D. Rodríguez-Gómez and G. Zafrir, *Discrete θ and the 5d superconformal index*, *JHEP* **01** (2014) 079 [[arXiv:1310.2150](#)] [[INSPIRE](#)].
- [8] O. Bergman, D. Rodríguez-Gómez and G. Zafrir, *5-Brane Webs, Symmetry Enhancement, and Duality in 5d Supersymmetric Gauge Theory*, *JHEP* **03** (2014) 112 [[arXiv:1311.4199](#)] [[INSPIRE](#)].
- [9] O. Bergman and G. Zafrir, *Lifting 4d dualities to 5d*, *JHEP* **04** (2015) 141 [[arXiv:1410.2806](#)] [[INSPIRE](#)].
- [10] O. Bergman and G. Zafrir, *5d fixed points from brane webs and O7-planes*, *JHEP* **12** (2015) 163 [[arXiv:1507.03860](#)] [[INSPIRE](#)].
- [11] S.-S. Kim, M. Taki and F. Yagi, *Tao Probing the End of the World*, *Prog. Theor. Exp. Phys.* **2015** (2015) 083B02 [[arXiv:1504.03672](#)] [[INSPIRE](#)].
- [12] G. Zafrir, *Brane webs and O5-planes*, *JHEP* **03** (2016) 109 [[arXiv:1512.08114](#)] [[INSPIRE](#)].
- [13] H. Hayashi, S.-S. Kim, K. Lee, M. Taki and F. Yagi, *More on 5d descriptions of 6d SCFTs*, *JHEP* **10** (2016) 126 [[arXiv:1512.08239](#)] [[INSPIRE](#)].
- [14] G. Zafrir, *Brane webs, 5d gauge theories and 6d $\mathcal{N} = (1, 0)$ SCFT's*, *JHEP* **12** (2015) 157 [[arXiv:1509.02016](#)] [[INSPIRE](#)].
- [15] H. Hayashi, S.-S. Kim, K. Lee and F. Yagi, *6d SCFTs, 5d Dualities and Tao Web Diagrams*, *JHEP* **05** (2019) 203 [[arXiv:1509.03300](#)] [[INSPIRE](#)].
- [16] G. Zafrir, *Brane webs in the presence of an O5⁻-plane and 4d class S theories of type D*, *JHEP* **07** (2016) 035 [[arXiv:1602.00130](#)] [[INSPIRE](#)].
- [17] H. Hayashi, S.-S. Kim, K. Lee and F. Yagi, *Equivalence of several descriptions for 6d SCFT*, *JHEP* **01** (2017) 093 [[arXiv:1607.07786](#)] [[INSPIRE](#)].
- [18] H. Hayashi and G. Zoccarato, *Partition functions of web diagrams with an O7⁻-plane*, *JHEP* **03** (2017) 112 [[arXiv:1609.07381](#)] [[INSPIRE](#)].
- [19] H. Hayashi and K. Ohmori, *5d/6d DE instantons from trivalent gluing of web diagrams*, *JHEP* **06** (2017) 078 [[arXiv:1702.07263](#)] [[INSPIRE](#)].

- [20] H. Hayashi, S.-S. Kim, K. Lee and F. Yagi, *Discrete theta angle from an O5-plane*, *JHEP* **11** (2017) 041 [[arXiv:1707.07181](#)] [[INSPIRE](#)].
- [21] H. Hayashi, S.-S. Kim, K. Lee and F. Yagi, *5-brane webs for 5d $\mathcal{N} = 1$ G_2 gauge theories*, *JHEP* **03** (2018) 125 [[arXiv:1801.03916](#)] [[INSPIRE](#)].
- [22] H. Hayashi, S.-S. Kim, K. Lee and F. Yagi, *Dualities and 5-brane webs for 5d rank 2 SCFTs*, *JHEP* **12** (2018) 016 [[arXiv:1806.10569](#)] [[INSPIRE](#)].
- [23] H. Hayashi, S.-S. Kim, K. Lee and F. Yagi, *Rank-3 antisymmetric matter on 5-brane webs*, *JHEP* **05** (2019) 133 [[arXiv:1902.04754](#)] [[INSPIRE](#)].
- [24] H.-C. Kim, M. Kim, S.-S. Kim and K.-H. Lee, *Bootstrapping BPS spectra of 5d/6d field theories*, *JHEP* **04** (2021) 161 [[arXiv:2101.00023](#)] [[INSPIRE](#)].
- [25] H.-C. Kim, S.-S. Kim and K. Lee, *Gauging \mathbb{Z}_N Discrete Symmetry of 5d SCFTs*, [arXiv:2112.14550](#) [[INSPIRE](#)].
- [26] M.R. Douglas, S.H. Katz and C. Vafa, *Small instantons, del Pezzo surfaces and type-I-prime theory*, *Nucl. Phys. B* **497** (1997) 155 [[hep-th/9609071](#)] [[INSPIRE](#)].
- [27] D.R. Morrison and N. Seiberg, *Extremal transitions and five-dimensional supersymmetric field theories*, *Nucl. Phys. B* **483** (1997) 229 [[hep-th/9609070](#)] [[INSPIRE](#)].
- [28] P. Jefferson, S. Katz, H.-C. Kim and C. Vafa, *On Geometric Classification of 5d SCFTs*, *JHEP* **04** (2018) 103 [[arXiv:1801.04036](#)] [[INSPIRE](#)].
- [29] C. Closset, M. Del Zotto and V. Saxena, *Five-dimensional SCFTs and gauge theory phases: an M-theory/type IIA perspective*, *SciPost Phys.* **6** (2019) 052 [[arXiv:1812.10451](#)] [[INSPIRE](#)].
- [30] L. Bhardwaj, *On the classification of 5d SCFTs*, *JHEP* **09** (2020) 007 [[arXiv:1909.09635](#)] [[INSPIRE](#)].
- [31] F. Apruzzi, S. Schäfer-Nameki and Y.-N. Wang, *5d SCFTs from Decoupling and Gluing*, *JHEP* **08** (2020) 153 [[arXiv:1912.04264](#)] [[INSPIRE](#)].
- [32] L. Bhardwaj and G. Zafrir, *Classification of 5d $\mathcal{N} = 1$ gauge theories*, *JHEP* **12** (2020) 099 [[arXiv:2003.04333](#)] [[INSPIRE](#)].
- [33] J. Tian and Y.-N. Wang, *5D and 6D SCFTs from \mathbb{C}^3 orbifolds*, *SciPost Phys.* **12** (2022) 127 [[arXiv:2110.15129](#)] [[INSPIRE](#)].
- [34] B. Acharya, N. Lambert, M. Najjar, E.E. Svanes and J. Tian, *Gauging discrete symmetries of T_N -theories in five dimensions*, *JHEP* **04** (2022) 114 [[arXiv:2110.14441](#)] [[INSPIRE](#)].
- [35] O. Bergman, D. Rodríguez-Gómez and C.F. Uhlemann, *Testing AdS_6/CFT_5 in Type IIB with stringy operators*, *JHEP* **08** (2018) 127 [[arXiv:1806.07898](#)] [[INSPIRE](#)].
- [36] M. Fluder and C.F. Uhlemann, *Precision Test of AdS_6/CFT_5 in Type IIB String Theory*, *Phys. Rev. Lett.* **121** (2018) 171603 [[arXiv:1806.08374](#)] [[INSPIRE](#)].
- [37] J. Kaidi and C.F. Uhlemann, *M-theory curves from warped AdS_6 in Type IIB*, *JHEP* **11** (2018) 175 [[arXiv:1809.10162](#)] [[INSPIRE](#)].
- [38] C.F. Uhlemann, *AdS_6/CFT_5 with O7-planes*, *JHEP* **04** (2020) 113 [[arXiv:1912.09716](#)] [[INSPIRE](#)].
- [39] C.F. Uhlemann, *Exact results for 5d SCFTs of long quiver type*, *JHEP* **11** (2019) 072 [[arXiv:1909.01369](#)] [[INSPIRE](#)].

- [40] A. Legramandi and C. Núñez, *Electrostatic description of five-dimensional SCFTs*, *Nucl. Phys. B* **974** (2022) 115630 [[arXiv:2104.11240](#)] [[INSPIRE](#)].
- [41] A. Legramandi and C. Núñez, *Holographic description of $SCFT_5$ compactifications*, *JHEP* **02** (2022) 010 [[arXiv:2109.11554](#)] [[INSPIRE](#)].
- [42] J. Gray, A. Hanany, Y.-H. He, V. Jejjala and N. Mekareeya, *SQCD: A Geometric Apercu*, *JHEP* **05** (2008) 099 [[arXiv:0803.4257](#)] [[INSPIRE](#)].
- [43] A. Hanany and N. Mekareeya, *Counting Gauge Invariant Operators in SQCD with Classical Gauge Groups*, *JHEP* **10** (2008) 012 [[arXiv:0805.3728](#)] [[INSPIRE](#)].
- [44] A. Sen, *F theory and orientifolds*, *Nucl. Phys. B* **475** (1996) 562 [[hep-th/9605150](#)] [[INSPIRE](#)].
- [45] M.R. Gaberdiel and B. Zwiebach, *Exceptional groups from open strings*, *Nucl. Phys. B* **518** (1998) 151 [[hep-th/9709013](#)] [[INSPIRE](#)].
- [46] M.R. Gaberdiel, T. Hauer and B. Zwiebach, *Open string-string junction transitions*, *Nucl. Phys. B* **525** (1998) 117 [[hep-th/9801205](#)] [[INSPIRE](#)].
- [47] O. DeWolfe, T. Hauer, A. Iqbal and B. Zwiebach, *Uncovering the symmetries on $[p, q]$ seven-branes: Beyond the Kodaira classification*, *Adv. Theor. Math. Phys.* **3** (1999) 1785 [[hep-th/9812028](#)] [[INSPIRE](#)].
- [48] O. DeWolfe, T. Hauer, A. Iqbal and B. Zwiebach, *Uncovering infinite symmetries on $[p, q]$ 7-branes: Kac-Moody algebras and beyond*, *Adv. Theor. Math. Phys.* **3** (1999) 1835 [[hep-th/9812209](#)] [[INSPIRE](#)].
- [49] O. DeWolfe, A. Hanany, A. Iqbal and E. Katz, *Five-branes, seven-branes and five-dimensional E_n field theories*, *JHEP* **03** (1999) 006 [[hep-th/9902179](#)] [[INSPIRE](#)].
- [50] H.-C. Kim, S.-S. Kim and K. Lee, *5-dim Superconformal Index with Enhanced E_n Global Symmetry*, *JHEP* **10** (2012) 142 [[arXiv:1206.6781](#)] [[INSPIRE](#)].
- [51] O. Bergman, D. Rodríguez-Gómez and G. Zafrir, *5d superconformal indices at large N and holography*, *JHEP* **08** (2013) 081 [[arXiv:1305.6870](#)] [[INSPIRE](#)].
- [52] C. Hwang, J. Kim, S. Kim and J. Park, *General instanton counting and 5d SCFT*, *JHEP* **07** (2015) 063 [*Addendum* *JHEP* **04** (2016) 094] [[arXiv:1406.6793](#)] [[INSPIRE](#)].
- [53] S.H. Katz and C. Vafa, *Matter from geometry*, *Nucl. Phys. B* **497** (1997) 146 [[hep-th/9606086](#)] [[INSPIRE](#)].
- [54] E. Witten, *Phase transitions in M-theory and F-theory*, *Nucl. Phys. B* **471** (1996) 195 [[hep-th/9603150](#)] [[INSPIRE](#)].
- [55] F. Apruzzi, C. Lawrie, L. Lin, S. Schäfer-Nameki and Y.-N. Wang, *Fibers add Flavor. Part I. Classification of 5d SCFTs, Flavor Symmetries and BPS States*, *JHEP* **11** (2019) 068 [[arXiv:1907.05404](#)] [[INSPIRE](#)].
- [56] F. Apruzzi, C. Lawrie, L. Lin, S. Schäfer-Nameki and Y.-N. Wang, *Fibers add Flavor. Part II. 5d SCFTs, Gauge Theories, and Dualities*, *JHEP* **03** (2020) 052 [[arXiv:1909.09128](#)] [[INSPIRE](#)].
- [57] L. Bhardwaj, *Flavor symmetry of 5d SCFTs. Part I. General setup*, *JHEP* **09** (2021) 186 [[arXiv:2010.13230](#)] [[INSPIRE](#)].
- [58] L. Bhardwaj, *Flavor symmetry of 5d SCFTs. Part II. Applications*, *JHEP* **04** (2021) 221 [[arXiv:2010.13235](#)] [[INSPIRE](#)].

- [59] G. Ferlito, A. Hanany, N. Mekareeya and G. Zafrir, *3d Coulomb branch and 5d Higgs branch at infinite coupling*, *JHEP* **07** (2018) 061 [[arXiv:1712.06604](#)] [[INSPIRE](#)].
- [60] M. Akhond, F. Carta, S. Dwivedi, H. Hayashi, S.-S. Kim and F. Yagi, *Five-brane webs, Higgs branches and unitary/orthosymplectic magnetic quivers*, *JHEP* **12** (2020) 164 [[arXiv:2008.01027](#)] [[INSPIRE](#)].
- [61] M. Akhond, F. Carta, S. Dwivedi, H. Hayashi, S.-S. Kim and F. Yagi, *Factorised 3d $\mathcal{N} = 4$ orthosymplectic quivers*, *JHEP* **05** (2021) 269 [[arXiv:2101.12235](#)] [[INSPIRE](#)].
- [62] M. Akhond and F. Carta, *Magnetic quivers from brane webs with $O7^+$ -planes*, *JHEP* **10** (2021) 014 [[arXiv:2107.09077](#)] [[INSPIRE](#)].
- [63] M. van Beest, A. Bourget, J. Eckhard and S. Schäfer-Nameki, *(5d RG-flow) Trees in the Tropical Rain Forest*, *JHEP* **03** (2021) 241 [[arXiv:2011.07033](#)] [[INSPIRE](#)].
- [64] M. van Beest, A. Bourget, J. Eckhard and S. Schäfer-Nameki, *(Symplectic) Leaves and (5d Higgs) Branches in the Poly(go)nesian Tropical Rain Forest*, *JHEP* **11** (2020) 124 [[arXiv:2008.05577](#)] [[INSPIRE](#)].
- [65] M. van Beest and S. Giacomelli, *Connecting 5d Higgs branches via Fayet-Iliopoulos deformations*, *JHEP* **12** (2021) 202 [[arXiv:2110.02872](#)] [[INSPIRE](#)].
- [66] A. Bourget, S. Cabrera, J.F. Grimminger, A. Hanany and Z. Zhong, *Brane Webs and Magnetic Quivers for SQCD*, *JHEP* **03** (2020) 176 [[arXiv:1909.00667](#)] [[INSPIRE](#)].
- [67] A. Bourget, J.F. Grimminger, A. Hanany, M. Sperling, G. Zafrir and Z. Zhong, *Magnetic quivers for rank 1 theories*, *JHEP* **09** (2020) 189 [[arXiv:2006.16994](#)] [[INSPIRE](#)].
- [68] A. Bourget, J.F. Grimminger, A. Hanany, M. Sperling and Z. Zhong, *Magnetic Quivers from Brane Webs with $O5$ Planes*, *JHEP* **07** (2020) 204 [[arXiv:2004.04082](#)] [[INSPIRE](#)].
- [69] A. Bourget, S. Giacomelli, J.F. Grimminger, A. Hanany, M. Sperling and Z. Zhong, *S-fold magnetic quivers*, *JHEP* **02** (2021) 054 [[arXiv:2010.05889](#)] [[INSPIRE](#)].
- [70] A. Bourget, J.F. Grimminger, A. Hanany, R. Kalveks, M. Sperling and Z. Zhong, *Magnetic Lattices for Orthosymplectic Quivers*, *JHEP* **12** (2020) 092 [[arXiv:2007.04667](#)] [[INSPIRE](#)].
- [71] A. Bourget, J.F. Grimminger, A. Hanany, R. Kalveks, M. Sperling and Z. Zhong, *Folding orthosymplectic quivers*, *JHEP* **12** (2021) 070 [[arXiv:2107.00754](#)] [[INSPIRE](#)].
- [72] C. Closset, S. Giacomelli, S. Schäfer-Nameki and Y.-N. Wang, *5d and 4d SCFTs: Canonical Singularities, Trinions and S-Dualities*, *JHEP* **05** (2021) 274 [[arXiv:2012.12827](#)] [[INSPIRE](#)].
- [73] C. Closset, S. Schäfer-Nameki and Y.-N. Wang, *Coulomb and Higgs Branches from Canonical Singularities. Part 0*, *JHEP* **02** (2021) 003 [[arXiv:2007.15600](#)] [[INSPIRE](#)].
- [74] S. Cabrera, A. Hanany and M. Sperling, *Magnetic quivers, Higgs branches, and 6d $N = (1, 0)$ theories*, *JHEP* **06** (2019) 071 [Erratum *JHEP* **07** (2019) 137] [[arXiv:1904.12293](#)] [[INSPIRE](#)].
- [75] S. Cabrera, A. Hanany and M. Sperling, *Magnetic quivers, Higgs branches, and 6d $\mathcal{N} = (1, 0)$ theories — orthogonal and symplectic gauge groups*, *JHEP* **02** (2020) 184 [[arXiv:1912.02773](#)] [[INSPIRE](#)].
- [76] F. Carta, S. Giacomelli, N. Mekareeya and A. Mininno, *Conformal manifolds and 3d mirrors of Argyres-Douglas theories*, *JHEP* **08** (2021) 015 [[arXiv:2105.08064](#)] [[INSPIRE](#)].
- [77] F. Carta, S. Giacomelli, N. Mekareeya and A. Mininno, *Conformal manifolds and 3d mirrors of (D_n, D_m) theories*, *JHEP* **02** (2022) 014 [[arXiv:2110.06940](#)] [[INSPIRE](#)].

- [78] M. Sperling and Z. Zhong, *Balanced B and D-type orthosymplectic quivers — magnetic quivers for product theories*, *JHEP* **04** (2022) 145 [[arXiv:2111.00026](#)] [[INSPIRE](#)].
- [79] S. Cremonesi, A. Hanany and A. Zaffaroni, *Monopole operators and Hilbert series of Coulomb branches of 3d $\mathcal{N} = 4$ gauge theories*, *JHEP* **01** (2014) 005 [[arXiv:1309.2657](#)] [[INSPIRE](#)].
- [80] S. Cremonesi, A. Hanany, N. Mekareeya and A. Zaffaroni, *Coulomb branch Hilbert series and Hall-Littlewood polynomials*, *JHEP* **09** (2014) 178 [[arXiv:1403.0585](#)] [[INSPIRE](#)].
- [81] S. Cremonesi, A. Hanany, N. Mekareeya and A. Zaffaroni, *Coulomb branch Hilbert series and Three Dimensional Sicilian Theories*, *JHEP* **09** (2014) 185 [[arXiv:1403.2384](#)] [[INSPIRE](#)].
- [82] S. Cremonesi, G. Ferlito, A. Hanany and N. Mekareeya, *Coulomb Branch and The Moduli Space of Instantons*, *JHEP* **12** (2014) 103 [[arXiv:1408.6835](#)] [[INSPIRE](#)].
- [83] A. Hanany and R. Kalveks, *Highest Weight Generating Functions for Hilbert Series*, *JHEP* **10** (2014) 152 [[arXiv:1408.4690](#)] [[INSPIRE](#)].
- [84] V. Borokhov, A. Kapustin and X.-k. Wu, *Monopole operators and mirror symmetry in three-dimensions*, *JHEP* **12** (2002) 044 [[hep-th/0207074](#)] [[INSPIRE](#)].
- [85] D. Gaiotto and E. Witten, *S-duality of Boundary Conditions In $N = 4$ Super Yang-Mills Theory*, *Adv. Theor. Math. Phys.* **13** (2009) 721 [[arXiv:0807.3720](#)] [[INSPIRE](#)].
- [86] B. Assel and S. Cremonesi, *The Infrared Physics of Bad Theories*, *SciPost Phys.* **3** (2017) 024 [[arXiv:1707.03403](#)] [[INSPIRE](#)].
- [87] B. Assel and S. Cremonesi, *The Infrared Fixed Points of 3d $\mathcal{N} = 4$ $USp(2N)$ SQCD Theories*, *SciPost Phys.* **5** (2018) 015 [[arXiv:1802.04285](#)] [[INSPIRE](#)].
- [88] I. Yaakov, *Redeeming Bad Theories*, *JHEP* **11** (2013) 189 [[arXiv:1303.2769](#)] [[INSPIRE](#)].
- [89] G. Ferlito and A. Hanany, *A tale of two cones: the Higgs Branch of $Sp(n)$ theories with $2n$ flavours*, [arXiv:1609.06724](#) [[INSPIRE](#)].
- [90] S. Cabrera, A. Hanany and F. Yagi, *Tropical Geometry and Five Dimensional Higgs Branches at Infinite Coupling*, *JHEP* **01** (2019) 068 [[arXiv:1810.01379](#)] [[INSPIRE](#)].
- [91] M. Aghand, F. Carta, S. Dwivedi, H. Hayashi, S.-S. Kim and F. Yagi, *Hilbert series for bad theories*, to appear.
- [92] N. Seiberg and E. Witten, *Gauge dynamics and compactification to three-dimensions*, in proceedings of *Conference in Memory of Claude Itzykson*, Saclay, France, 5–7 June 1996, *Advanced Series in Mathematical Physics* **24**, J.M. Drouffe and J.B. Zuber eds., World Scientific, Singapore (1996), pp. 333–366 [[hep-th/9607163](#)] [[INSPIRE](#)].
- [93] A. Hanany and N. Mekareeya, *Complete Intersection Moduli Spaces in $N = 4$ Gauge Theories in Three Dimensions*, *JHEP* **01** (2012) 079 [[arXiv:1110.6203](#)] [[INSPIRE](#)].
- [94] O. Chacaltana and J. Distler, *Tinkertoys for Gaiotto Duality*, *JHEP* **11** (2010) 099 [[arXiv:1008.5203](#)] [[INSPIRE](#)].
- [95] O. Chacaltana and J. Distler, *Tinkertoys for the D_N series*, *JHEP* **02** (2013) 110 [[arXiv:1106.5410](#)] [[INSPIRE](#)].